A NEW FOURTH ORDER RESONANT DC-DC CONVERTER WITH PWM CONTROL

by

GYANENDRA DEV TRIPATHI

DEPARTMENT OF ELECTRICAL ENGINEERING

INDIAN INSTITUTE OF TECHNOLOGY KANPUR

September, 1998

A NEW FOURTH ORDER RESONANT DC-DC CONVERTER WITH PWM CONTROL

A Thesis Submitted

in Partial Fulfillment of the Requirements

for the Degree of

Master of Technology

by

GYANENDRA DEV TRIPATHI

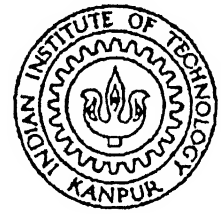

to the

DEPARTMENT OF ELECTRICAL ENGINEERING

INDIAN INSTITUTE OF TECHNOLOGY KANPUR

September 1998

Dedicated To

My Respected Parents

Smt. Rama Tripathi

And

Shri R.D. Tripathi

CERTIFICATE

It is certified that the work contained in the thesis entitled **A New Fourth Order Resonant DC-DC Converter with PWM Control**, by **Gyanendra Dev Tripathi**, has been carried out under my supervision and that this work has not been submitted elsewhere for a degree.

Dr. S.R.Doradla
Professor
Department of Electrical Engineering
Indian Institute of Technology
Kanpur

14 September, 1998

Abstract

Many of the limitations of two element resonant topologies can be overcome by adding the third reactive element. However,the number of possible circuit topologies increase as number of reactive elements increase.The selection of a proper higher order topology for a given application is a difficult task. In this work a new LC-LC type resonant converter using a capacitor output filter and providing load independent operation at two frequencies is presented. Pulsewidth modulation (PWM) is employed to control the output voltage. The possible modes of converter operation under PWM are analysed using state space equations with numerical solution approach.A new analysis technique by state varibale transformation and developing decoupled state space equation,is developed for frequency controlled converter. This method turns out to be an efficient analysis tool for higher order converters. Steady state solutions are obtained by running the simulations for sufficiently large times. Closed form solutions are worked out based on a simple analysis technique-Complex circuit analysis technique.

An extensive simulation has been carried out using a C Program which is compared with SPICE-software package for verification. The C program was used extensively to study the transient and steady state performance.There is complete agreement between the results obtained by the above program and those obtained by SPICE.

Acknowledgements

At first I would like to thank my learned supervisor Prof.(Dr.) S.R.Doradla, who has been constant source of inspiration for me. I can not forget the kind of academic freedom he catered to me in due course of this work. I will remain indebted to him for his morale boosting approach when I had some medical problems.

I would like to record my gratitude to Prof. G.K. Dubey,Prof. A.Joshi,Dr. V.R. Sule, Dr. B.G. Fernandez,Dr. G. Sharma,Dr. D. Manjunath for providing knowledge through their courses.

I am grateful to my great parents (specially my Mother) who have dedicated each and every resources they had at their disposal to make sure my success.

I feel happy to remember my friends Vivek,Pradeep,Vishnu,Shailendra,Narendra,Amit and many others who made my stay at IIT Kanpur a memorable one.

Last but not the least I would like to thank Mr. O.P.Arora of Power Electronics Lab who has provided all kind of help when I needed.

Gyanendra Dev Tripathi

Contents

Certificate iii

Abstract iv

Acknowledgment v

Contents vi

List of Figures viii

1 INTRODUCTION 1

1.1 Introduction 1

1.2 Literature Survey 2

1.2.1 Control Techniques of Resonant Converters 2

1.2.2 Analysis and Modelling Techniques 4

1.2.3 Topological Aspect 7

1.3 Scope of Present Work 7

1.3.1 Objective 7

1.4 Organisation of the Thesis 9

2 Analysis Of Fourth Order Converters 10

2.1 Introduction 10

2.2 Steady State Analysis 11

2.2.1 Time Domain Analysis 11
2.2.2 Complex Circuit Analysis Technique 25
2.2.3 Effect of Bridge Rectifier on the Value of Load Resistance . . . 25
2.2.4 Description Of the Technique 27
2.2.5 Calculation of Component Stresses 32

3 Selection of Topology **41**
3.1 Introduction 41
3.1.1 Selection Methodology 41
3.1.2 Selection of Operating Frequency 42
3.1.3 Optimisation of the Function 43

4 LCLC Converter **48**
4.1 Description of Circuit Functioning 48

5 Simulation Of the Converter **52**
5.1 Introduction 52
5.2 Design of the Converter Components 52
5.2.1 Selection of the Output Filter Capacitor C_O 54
5.3 Start-Up of the Converter 55
5.4 SPICE3 Simulation Methodology 55
5.5 Simulation by Transient Numerical Solution of Differential Equations . 58
5.5.1 Operation of the Converter with Pulsed Load 59

6 Conclusion **65**
6.1 Conclusion 65
6.2 Suggestions for Future Work 66

Bibliography **67**

Appendix A 70

Appendix B 76

List of Figures

2.1 Diffrent Topologies with Four elements(2 L and 2 C) and Voltage source and Voltage sink type(V-N-V) 12

2.2 Selected Topologies For Analysis with Four elements(2 L and 2 C) and Voltage source and Voltage sink type(V-N-V) 12

2.3 Block Diagram of General Resonant Converter (a) Full Bridge V-N-V (b) Half Bridge V-N-V (c) Equivalent circuit 13

2.4 Equivalent Circuit of the Converter(Topology 8) 14

2.5 Steady state Waveforms for the converter(Topology 8)($F1 < 1.0$). . . . 14

2.6 Steady state Waveforms for the converter(Topology 8)($F1 > 1.0$). . . . 15

2.7 Output Characterstics Curves of the converter of topology 6(a = 1,b = 1). 21

2.8 Output Characterstics Curves of the converter of topology 6(a = 2,b = 1) for different values of frequencies. 22

2.9 Output Characterstics Curves of the converter of topology 6(a = 1,b = 2). 23

2.10 Output Characterstics Curves of the converter of topology 6 (F1 = 0.9 with a and b varied. 24

2.11 Output characterstics by Simulation and analysis for $a = 2, b = 1$ and $F_1 = 0.92$. 25

2.12 Gain vs Frequency Curves for $a = 2$ and $b = 1$ Using Time Domain Analysis. 26

2.13 Gain vs Frequency Curves for $a = 2$ and $b = 2$ Using Time Domain Analysis. 27

2.14 Gain vs Frequency Curves for $a = 1$ and $b = 1$ Using Time Domain Analysis. 28

2.15 AC equivalent circuit of general resonant converter 29

2.16 Circuit diagram of output bridge rectifier and filter 29

2.17 The wave form of the inverter output voltage $v_{AB}(t)$. 30

2.18 AC equivalent circuit of topology 8. 30

2.19 Gain vs Normalised Switch Freq. Curves for Various Load Resistaces a=1,b=1 31

2.20 Gain vs Normalised Switch Freq. Curves for Various Load Resistaces a=2,b=1 32

2.21 Conveter Gain for Varying Duty Ratio (D),$Q_1 = 2$ 33

2.22 Normalised Peack values of different state variables by differential equation method and CCA method(Variables with subscript 1 represent those obtained by actual simulation whereas others are those found by CCA)(Topology 13). 35

2.23 Normalised Peack values of different state variables by differential equation method and CCA method(Variables with subscript 1 represent those obtained by actual simulation whereas others are those found by CCA)(Topology 2). 36

2.24 Normalised Peack values of different state variables by differential equation method and CCA method(Variables with subscript 1 represent those obtained by actual simulation whereas others are those found by CCA)(Topology 3). 37

2.25 Normalised Peack values of different state variables by differential equation method and CCA method(Variables with subscript 1 represent those obtained by actual simulation whereas others are those found by CCA)(Topology 5). 38

2.26 Normalised Peack values of different state variables by differential equation method and CCA method(Variables with subscript 1 represent those obtained by actual simulation whereas others are those found by CCA)(Topology 8). 39

2.27 Normalised Peack values of different state variables by differential equation method and CCA method(Variables with subscript 1 represent those obtained by actual simulation whereas others are those found by CCA)(Topology 7). 40

3.1 Value of Optimising function for different values of q,D=1, a = 0.5, b = 0.5. 43

3.2 Value of Optimising function for different values of q,D=1,a = 1, b = 1. 44

3.3 Value of Optimising function for different values of q,D=1,a = 2, b = 2. 45

3.4 Value of Optimising function for different values of q,D=1,a = 2, b = 1. 46

3.5 Value of Optimising function for different values of q,D=1,a = 1,b = 2. 47

4.1 The circuit diagram of a fourth order resonant converter 49

4.2 Switching (Gate) wave forms for the different switches of high frequency inverter. 50

4.3 Timing Diagram of the state variables(Normalised) of the conveter(Lagging pf mode 51

5.1 Transient response for the step change in the load resistance(from Q1=2.0 to Q1 = 4.0) with two different filter capacitors (dots for $\frac{C1}{C_o} = 0.035$ and lines for $\frac{C1}{C_o} = 0.0035$ 55

5.2 Transient response for the step change in duty ratio(from D=0.4 to D = 1.0) with two different filter capacitors (dots for $\frac{C1}{C_o} = 0.035$ and lines for $\frac{C1}{C_o} = 0.0035$ 56

5.3 Variation of percentage ripple in output voltage vs ratio $\frac{C1}{C_o}$ (Q1 = 2.0) 57

5.4 Start-up Transient response with two different filter capacitor initial voltages $\frac{C1}{C_o} = 0.035$ (dots for Mo = 1.0 and lines for Mo = 0.5) 58

5.5 Detailed Circuit Diagram of the Converter Used for SPICE3 Simulation(Topology 8) 59

5.6 Simulated wave forms for $Q_1 = 2.0(R_L = 25ohm)$ and D = 0.4. 60

5.7 Simulated wave forms for $Q_1 = 0.4(R_L = 125ohm)$ D = 0.4. 60

5.8 Simulated wave forms for $Q_1 = 2(R_L = 25ohm)$ D = 0.8. 61

5.9 Simulated wave forms for $Q_1 = 0.4(R_L = 125ohm)$ D = 0.8. 61

5.10 Simulated wave forms for $Q_1 = 2(R_L = 25ohm)$ D = 1.0. 62

5.11 Simulated wave forms for $Q_1 = 0.4(R_L = 125ohm)$ D = 1.0. 62

5.12 Simulation Waveforms of the Converter for $Q_1 = 2.0$,D = 0.75(Using C program). 63

5.13 Simulation Waveforms of the Converter for $Q_1 = 2.0$,D = 0.75(Using SPICE). 63

5.14 Simulated Waveforms of the State variables for Pulsed Load($Q_{1min} = 0.5, Q_{1max} = 2.0, D = 0.8$). 64

Chapter 1

INTRODUCTION

1.1 Introduction

The resonant converters have been enjoying the interests of researchers for quite a long time because of their following inherent qualities:

- lower size & weight of reactive components.
- high frequency of operation.
- less EMI.
- soft switching and hence lower switching losses.
- high efficiency.
- low harmonic content etc.

The research in this area has been multidirectional in nature. For having a overview regarding dimensions of the research,a literature review is presented in the following section.

1.2 Literature Survey

Resonant converter concept was first reported and patented by Schwarz [21] in 1976. In this seminal work the so called series resonant converter(later named as Schwarz conveter) is discussed in detail. It is shown in this paper that the power transfer from source to load through resonant tank can be controlled by controlling the phase angle (ψ_r) between input voltage and output voltage of resonant tank.

A control system known as "Analog Signal to Discrete Time Interval Converter" (ASDTIC) is also discussed and utilised for controlling the converter.

1.2.1 Control Techniques of Resonant Converters

The well known series resonant converter(SRC) and parallel resonant converter(PRC) have been analysed and investigated exhaustively in the open literature [20, 21, 28]. In these converters the output voltage is controlled by controlling the frequency of operation. In SRC the output voltage is load independent only if the operating frequency is very near to resonant frequency ,but we can not have voltage regulation in this case. So for varying loads we will have to change the frequency of operation over a very wide range. The PRC has a demerit that at lighter loads the efficiency of the converter decreases because of circulating currents. It also gives load dependent operation.

In an attempt to overcome the limitations of the converters listed above,fixed frquency control with various control techniques were tried.

- Fixed frequency with phase staggering control [12].
- Fixed frequency with pulsewidth strategy [19, 22].
- Integral cycle control(Quantum control) [14, 15].

1.2.1.1 Fixed Frequency Phase Staggering Control

Two resonant inverters are connected to a common load with a phase shift between the voltages of individual inverters. Summing of their output voltages or currents provides

nearly 100% range control. This strategy is extensively covered in [12] . The operation at light loads is quite satisfactory,but it has the following disadvantages.

- The number of switches are double that of normal SLRC. This results in more losses.
- Lower efficiency at lighter loads.
- The converter performance is still load dependent,for given phase and input voltage because the converters are not operated at resonant frequency.

1.2.1.2 Pulsewidth Control Strategy with Fixed Frequency

The resonant inverter is operated at fixed frequency and control is obtained by varying the pulsewidth of the bipolar switching waveform applied to the resonant tank network. Pulsewidth modulation solves completely the problem of loss of control at light loads [22] as the time during which the source is connected to resonant tank is reduced to almost zero. Also,by proper choice of switching frequency in relation to the resonant frequency,the turn on losses can be reduced to zero and the turn off losses can be minimised by the use of capacitive(lossless) snubbers. Though this strategy solves many problems,still the load dependent nature of the output voltage remains unsolved if the frequency of switching is not same as resonant frequency,and at times elaborate switching strategies are employed to control the output voltage under extreme load conditions.

1.2.1.3 Integral Cycle Control

In this mode of control, the resonant inverter is switched exactly at resonant frequency and the output voltage is controlled by time domain control i.e. by proper selection of switch modes - power mode and free resonant mode. In the power mode,the source power is delivered to resonant tank network and load. In the free resonant mode,switches are controlled in such away that the resonant tank supplies power to the load without drawing any power from the source. Importantly,the inverter is either of the modes for a complete half cycle of operation. By controlling the number of half cycles of power to the number of half cycles of free resonant in a interval of time period,

the output voltage is linearly controlled. This scheme overcomes all the disadvantages of other schemes. However,it has following limitations.

- Control within one half cycle is not possible.
- Response is slow as it depends on number of cycles in a given period.
- If the number of half cycles for a given period is low, then quantum step of output voltage is large.
- Peak stresses of the resonant tank components are high as the switching frequency is same as resonant frequency.

Other control techniques which have been utilised and reported are :

- Resonant tank control.[8]
- Optimal trajectory control.[6]
- Closed loop control with externally designed robust controllers.[7, 10, 16]

1.2.2 Analysis and Modelling Techniques

Analysis and modelling of the resonant converters is relatively difficult when it is compared with conventional PWM converters (Buck,Boost,Buck-boost,cu$\hat{k}$ converters etc.) because state space averaging technique-which proves to be a wonderful tool for modelling PWM converters,is not applicable because the internal circuit time constants are comparable to the switching frequency. Number of analysis and modelling techniques have been developed in the literature but still there is no technique which could establish its superiority over the remaining ones. Following are the techniques which have been reported in the literature:

- State-space numerical solution of steady state [21, 5, 20, 29].
- Sampled data modelling technique [9].
- State plane analysis technique [18, 16].

- Complex circuit analysis technique [26, 13, 24].
- Fourier series technique [27].

1.2.2.1 State-Space Numerical Solution of Steady State

In this the converter circuit is represented by a number of circuits describing each mode of operation seperately. Then state variables are solved for each mode and by applying the initial and boundry conditions the closed form solutions for different converter parameters are obtained.[20, 21, 5]

This technique is restricted to be used for converters where state variable are limited(not more than 3) in number. As the number of state variables goes high this techniques can not be applied easily.

Another drawback of this technique is that only steady state parameters are obtained and hence it is not suitable for transient analysis.

1.2.2.2 Sampled Data Modelling Technique

This technique utilises the inherent sampled nature of the switched converter and assumes that the converter switchings are possible only at discrete intervals. Each cycle of operation is divided into number of subintervals at which some condition or state of the circuit undergoes a change [9]. The boundry conditions are applied at the end of each subinterval and in this way the states at the end of cycle are related to the states at the start of the cycle and input conditions. In this way we get a sampled-data reperesentation of the system. The z-Transform technique and perturbation techniques are used to describe the behaviour of the system and small signal modelling of the system respectively [9].

Because the sampling frequency is same as the switching frequency hence this method gives satisfactory results only if the control signals are changing at a frequency which is less than half of the switch frequency.

1.2.2.3 State-Plane Analysis Technique

This is a graphical technique in which the converter state variables are normalised and represented on a state plane and different control methods are also represented by control characterstics on the same plane and the converter parameters are evaluated once the state plane parameters are determined. A general method for analysing parallel resonant converters with state plane is suggested in [3]. This method is simple for simple converters(SRC or PRC) but becomes very involved if number of state variables are more than two [4, 3]. A control method known as Optimal Trajectory Control is discussed in [6].

1.2.2.4 Complex Circuit Analysis Technique

This technique is quite simple but applicable only in a limited range of frequencies around the resonant frequency of the converter. In this the converter is assumed to be fed by a sinusoidal voltage source which is equal to the fundamental component of the inverter output voltage. The load is replaced by an equivalent resistance. This technique is largely described in chapter 2.

1.2.2.5 Fourier Series Method

This technique of analysing the resonant converters is based on the fact that inverter output voltage can be represented by its Fourier Series description and similarily the the output voltage or current can also be represented by Fourier series. The circuit performance is calculated as a response to these two energy sources and sinks and by applying energy conservation law the conveter parameters are evaluated. This technique is described for SRC in [27].

This technique is quite accurate as we can choose as many harmonics as we please for analysis.

1.2.3 Topological Aspect

It has been shown in [5, 11, 13] that the demerits of converters with two elements can be eliminated,while maintaining the properties of original converters,by the addition of the third element(e.g. LCC,LCL,LLC converters etc.). Some reserchers have recently started showing their interest in higher order topologies.

The converters of two.three.and fourth order commutation networks are listed in [13]. There are 98 topologies possible with 4 elements(2 inductor and 2 capacitor). The fourth order topologies are more representative because they can make use of transformer parasitics profitably [25, 13]. In [19] the series resonant converter with anothe parallel branch(LC-LC) is analysed and shown to be more efficient. In [24] a new control method by switching from one resonant frequency to another out of the three resonant frequencies of a high order convrter is presented and hence converter always function with zero current switching(ZCS) at three power levels. The advantages of higher order converters have not been fully explored so far and number of works are being reported on this topic.

1.3 Scope of Present Work

1.3.1 Objective

The main objective is to study the fourth order DC-DC V-N-V converters [13]. The study involves analysis,selection of Topology with minimum component stresses and simulation of the converter. The possible applications envisaged for the proposed converter are:

- High voltage power supplies used in communication equipments such as radars.
- DC-DC converters used in airborne/space applications.
- Industrial applications such as induction heating.

1.3.1.1 High Voltage Power Supplies[25]

High voltage power supplies are required in radar transmitter to energise the final power amplifier. In most of the pulsed radars the load to these power supplies is pulsed in nature. Therefore,large capacitance filters are generally used at the output and peak currents of the order of 10 A to 30 A is drawn for short duration depending on the pulsewidth and duty ratio of the radar system. The pulsewidth generally ranges from 1 μs to 30 μs and pulse repetition frequencies(PRFs) from 500 Hz - 10 kHz. Therefore,the DC-DC converters used to generate high voltage should be capable of working with capacitive filters(voltage-source loads) . The PRF is generally changed very frequently. This demands that the converter should be capable of working varying loads.

It has been pointed out[29] that main problems associated with the DC-DC converter used for HV power supplies are parasitic reactive elements associated with HF transformer.

It has been suggested [29] that an attractive alternative for HV DC-DC applications is the use of resonant converter in which the transformer non idealities are incorporated into basic operation of the circuit.

1.3.1.2 DC-DC convertes used in space application[25]

DC-DC converters are used in airborne equipment to convert the 48V DC into required voltage lavels necessary for operating various electronic equipments. The important requirements for these applications are:

- Small size and light weight.
- Reliability of equipment.
- Less EMI.
- Easy control.

1.3.1.3 DC-DC Converters for Induction Heating[25]

The load on induction heating equipment depends on the size of the job. Hence the converter used for this application should take varying loads. Therefore,a load insensitive output voltage is always preferred for this application.

In present work the characterstics of fourth order resonant converters are investigated and a method for selecting the right topology is discussed. The selected topology is exaustively simulated using SPICE3 and a C program is written to carry out the transient analysis of the converter to study the behaviour of the converter at starting and for step changes in control parameter(D) or load(Q_1). The design method and selection of optimum filter capacitor is also described in detail.

A new steady state analysis technique is developed using state variable transformation and is verified by simulation results.

The start-up of the converter is discussed in detail so that optimal starting of the converter can be assured without much stresses on the components.

1.4 Organisation of the Thesis

The present work is organised in six chapters.

Chapter 1 gives a brief literature review and introduction of the work done so far on the resonant converters. Chapter 2 gives detailed analysis of the fourth order V-N-V converters with example of a topology. In chapter 3 the discussion related to the selection of the suitable fourth order topology is presented. The minimum component stresses principle is also discussed. Chapter 4 presents the operation of the selected fourth order converter. In chapter 5 detailed simulation of converter is presented with the methodology adopted for the simulation. Chapter 6 gives a brief conclusion of the present work and suggestions for the further work on this topic.

Chapter 2

Analysis Of Fourth Order Converters

2.1 Introduction

As the number of state variables increases in a switched converter,the state space analysis and closed form solutions become difficult to obtain. In a switched converter there is always a switching non-linearity and hence piece-wise wave form equations can be obtained but applying boundry conditions in a higher order system to achieve the closed form solutions is a difficult(sometimes impossible) task because it requires iterative solutions of the initial and boundry conditions.

There are 98 possible topologies with 4-elements (2 inductors and 2 capacitors) [13]. Out of which 16 are pointed to be of voltage source and voltage sink type. These topologies are listed in fig 2.1. Out of these 16 topologies 4 are just shunt type and they are not considered because in these there is no control of output voltage (which always remains same as that of the input voltage). Out of remaining 12 topologies those topologies are considered in which the leakage inductance of the transformer can be added into one of the resonant inductors . Hence only 6 topologies which are described in appendix-A are used for further study. These are listed in fig. 2.2.

A practical method for steady state analysis of fourth order resonant DC-DC converter is presented. In this method the converter is represented by the differential equations for each state variable. Then state variable are transformed to a new set

of variables as suggested in [3] so that the new state equations are completely decoupled. Now the new state equations are solved and transformed back to original state variables. Now by applying the initial and boundry conditions the parameters of the conveter are computed.

A simple complex circuit analysis(CCA) technique is suggested in literature [13] and used profitably [26] for analysis of resonant converters. This technique turns out to be a wonderful tool if the switching frequency of the converter is close to or above the resonant frequency of the system [17]. This is not really a restriction,as in practice ,a converter is normally driven close to or above resonance frequency to achieve better efficiency [25].

For validating the results obtained by CCA technique , the actual state space equations are solved numerically with the help of a computer and different parameters (converter gain and peak component stresses etc) are obtained by both the methods are compared and found to be matching.

2.2 Steady State Analysis

The general block diagram an equivalent circuit of N^{th} order resonant converter is shown in fig. 2.3 and the networks shown in fig 2.2 are substituted in place of the "n^{th} order resonant tank" block to get the converters of different possible topologies. The steady state analysis can be carried out with Time domain analysis as well as complex circuit analysis. The methods of analysis are presented only for topology 8,for the sake of presentational ease.

2.2.1 Time Domain Analysis

In general,the derivation of analytical equations for resonant converters must begin with the state-space model. Following assumptions are used to simplify the analysis.

- All the devices and components are ideal.
- Filter capacitor is very large so that the output voltage remains constant in steady state.

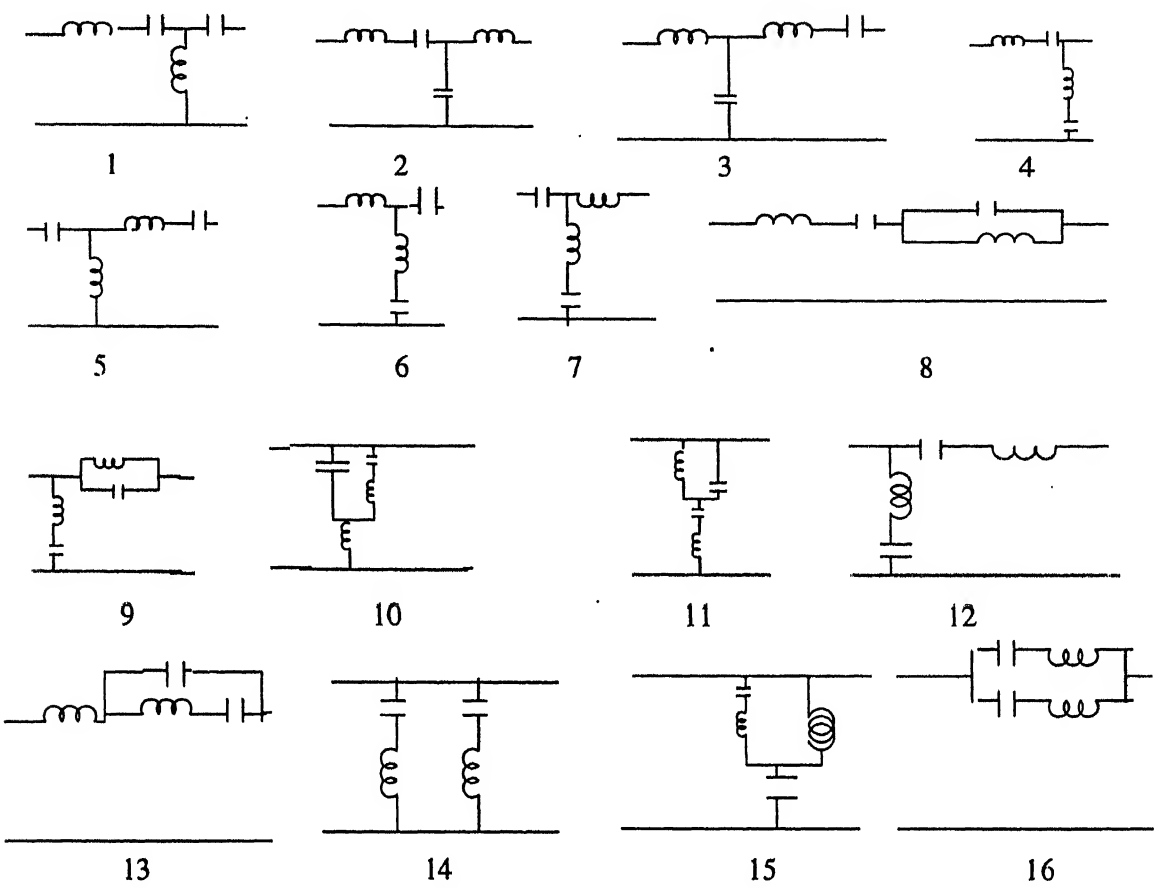

Figure 2.1: Diffrent Topologies with Four elements(2 L and 2 C) and Voltage source and Voltage sink type(V-N-V)

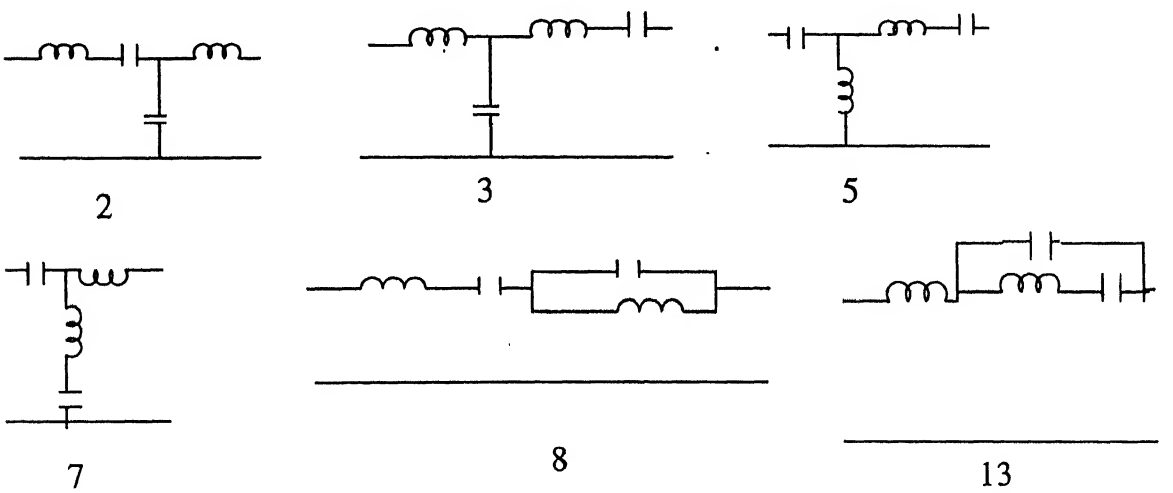

Figure 2.2: Selected Topologies For Analysis with Four elements(2 L and 2 C) and Voltage source and Voltage sink type(V-N-V)

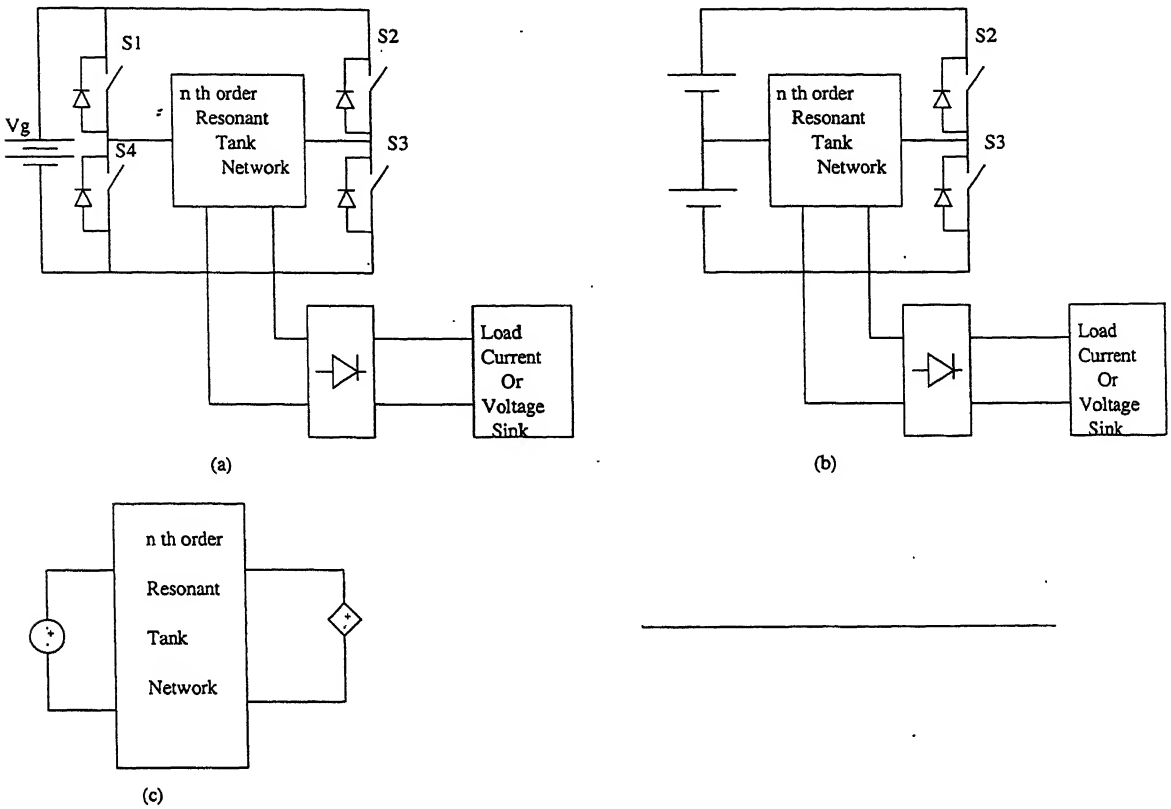

Figure 2.3: Block Diagram of General Resonant Converter (a) Full Bridge V-N-V (b) Half Bridge V-N-V (c) Equivalent circuit

- The duty cycles of the gate signals for switches S1,S3 and S2,S4 are 50% each and non-overlapping.

fig. 2.19 and the steady state differential equations are given in eq. 2.1- 2.4.

Based on the above assumptions and the equivalent circuit of fig. 2.4 the steady state waveforms of fig. 2.5 and fig. 2.6 are used to find a state space model as given by eq. 2.1- 2.4.

$$\frac{di_{L1}}{dt} = -\frac{1}{L1}\left(v_{C1} + v_{C2} + sgn(i_{L1}).V_o - mV_g\right) \tag{2.1}$$

$$\frac{dv_{C1}}{dt} = \frac{1}{C1} i_{L1} \tag{2.2}$$

$$\frac{di_{L2}}{dt} = \frac{1}{L2} v_{C2} \tag{2.3}$$

$$\frac{dv_{C2}}{dt} = \frac{1}{C2}\left(i_{L1} - i_{L2}\right) \tag{2.4}$$

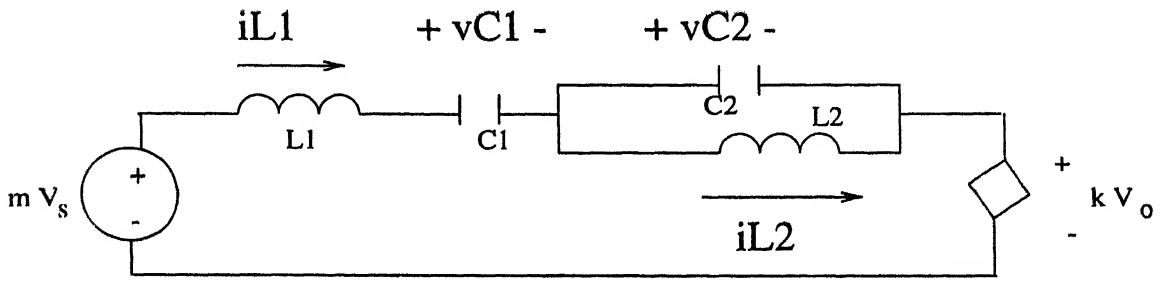

Figure 2.4: Equivalent Circuit of the Converter(Topology 8)

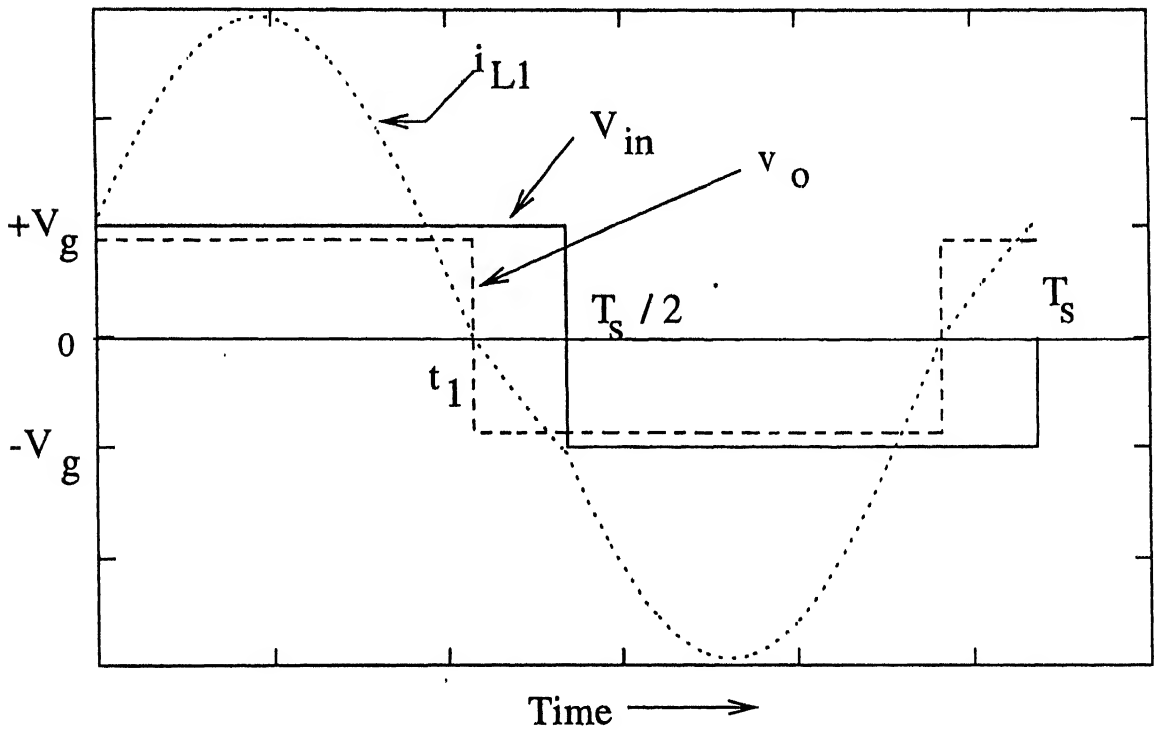

Figure 2.5: Steady state Waveforms for the converter(Topology 8)($F1 < 1.0$).

Let the transformed variables are defined as given by eq. 2.5- 2.8.

$$v_1 = v_{C1} + K_1 v_{C2} \tag{2.5}$$

$$v_2 = v_{C1} + K_2 v_{C2} \tag{2.6}$$

$$i_1 = i_{L1} + K_3 i_{L2} \tag{2.7}$$

$$i_2 = i_{L1} + K_4 i_{L2} \tag{2.8}$$

where K_1-K_4 are defined as given by eq. 2.9- 2.12.

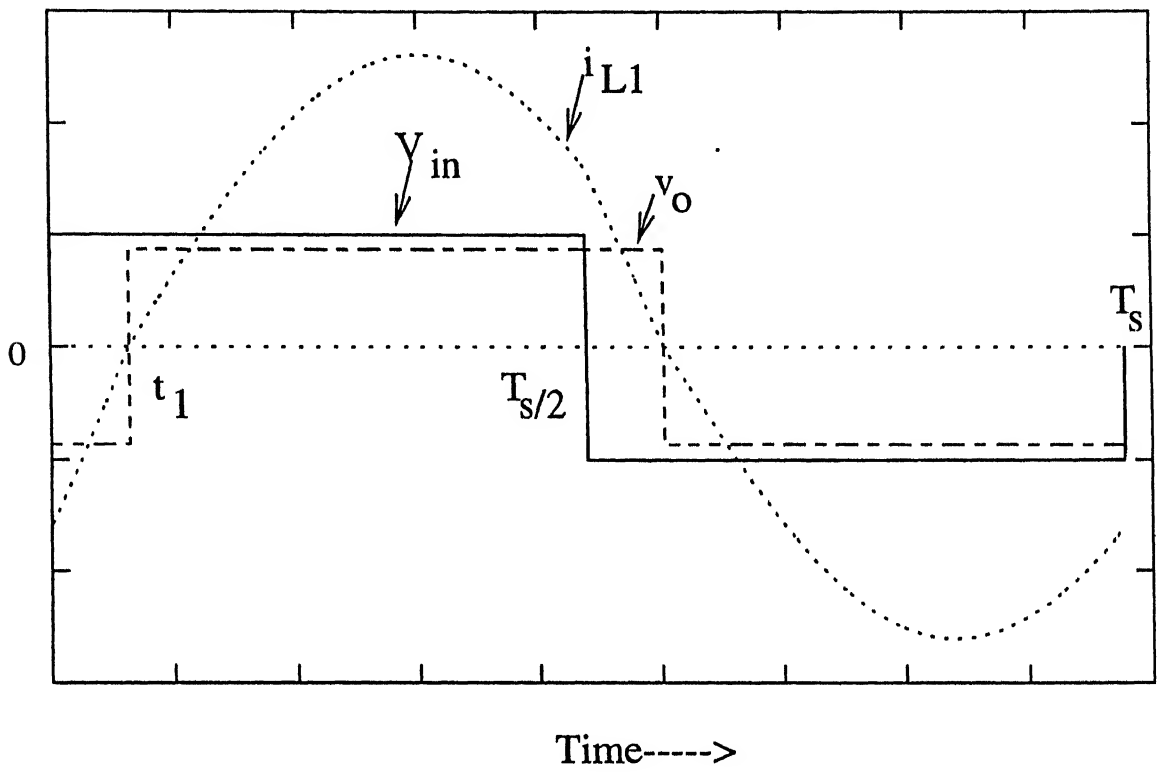

Figure 2.6: Steady state Waveforms for the converter(Topology 8)($F1 > 1.0$).

$$K_1 = \frac{(1+b-a) + \sqrt{(1+b-a)^2 + 4a}}{2} \tag{2.9}$$

$$K_2 = \frac{(1+b-a) - \sqrt{(1+b-a)^2 + 4a}}{2} \tag{2.10}$$

$$K_3 = \frac{1-K_1}{b} \tag{2.11}$$

$$K_4 = \frac{1-K_2}{b} \tag{2.12}$$

where a and b are defined as follows:

$$a = \frac{C2}{C1} \tag{2.13}$$

$$b = \frac{L1}{L2} \tag{2.14}$$

The state equations in transformed variables are given by eq. 2.15- 2.18

$$\frac{di_1}{dt} = -\frac{1}{L1}(v_1 + sgn(i_{L1}).V_o - mV_g) \tag{2.15}$$

$$\frac{dv_1}{dt} = \frac{1}{C11} i_1 \tag{2.16}$$

$$\frac{di_2}{dt} = -\frac{1}{L1}(v_2 + sgn(i_{L1}).V_o - mV_g) \tag{2.17}$$

$$\frac{dv_2}{dt} = \frac{1}{C12} i_2 \tag{2.18}$$

where C11 and C12 are defined as following:

$$C11 = \frac{C2}{(a1 + K_1)} \tag{2.19}$$

$$C12 = \frac{C2}{(a + K_2)} \tag{2.20}$$

Now the state equations given by eq. 2.15- 2.16 are normalised by the base quantities given as following.

$V_B = V_g$

$Z_{B1} = \sqrt{\frac{L1}{C11}}$

$I_{B1} = \frac{V_B}{Z_B 1}$

$\omega_{B1} = \frac{1}{\sqrt{L1C11}}$

whereas the eq. 2.17- 2.18 are normalised by the base quantities as following.

$V_B = V_g$

$Z_{B2} = \sqrt{\frac{L1}{C12}}$

$I_{B2} = \frac{V_B}{Z_B 2}$

$\omega_{B2} = \frac{1}{\sqrt{L1C12}}$

Normalised state equations are given by eq. 2.21- 2.24.

$$\frac{dj_1}{d\theta_1} = -(m_1 + sgn(i_{L1}).M - m) \tag{2.21}$$

$$\frac{dm_1}{d\theta_1} = j_1 \tag{2.22}$$

$$\frac{dj_2}{d\theta_2} = -(m_2 + sgn(i_{L1}).M - m) \tag{2.23}$$

$$\frac{dm_2}{d\theta_2} = j_2 \tag{2.24}$$

where θ_1 and θ_2 are defined as following:

$$\theta_1 = \omega_{B1} t \tag{2.25}$$

$$\theta_2 = \omega_{B2} t \tag{2.26}$$

we define the ratio of two resonant frequencies ω_{21} as following:

$$\omega_{21} = \frac{\omega_{B2}}{\omega_{B1}} \tag{2.27}$$

$$\omega_{21} = \sqrt{\frac{(K_2 + a)}{(K_1 + a)}} \tag{2.28}$$

2.2.1.1 General Solutions of the Decoupled Equations

The general solutions to the eq. 2.18- 2.24 can be obtained very easily and are given by eq. 2.29- 2.32.

$$m_1(\theta_1) = A_1 cos(\theta_1) + B_1 sin(\theta_1) + (m - sgn(i_{L1})M) \tag{2.29}$$

$$j_1(\theta_1) = B_1 cos(\theta_1) - A_1 sin(\theta_1) \tag{2.30}$$

$$m_2(\theta_2) = A_2 cos(\theta_2) + B_2 sin(\theta_2) + (m - sgn(i_{L1})M) \tag{2.31}$$

$$j_2(\theta_2) = B_2 cos(\theta_2) - A_2 sin(\theta_2) \tag{2.32}$$

where A_1,A_2,B_1 and B_2 can be obtained by applying the initial conditions in eq. 2.29-2.32.

2.2.1.2 Solutions for Different Time Intervals

The solutions for time interval P1($\alpha_1 > \theta_1 > 0$):

$$m_1(\theta_1) = (m_{10} + M - 1)cos(\theta_1) + j_{10}sin(\theta_1) + (1 - M) \tag{2.33}$$

$$j_1(\theta_1) = j_{10}cos(\theta_1) - (m_{10} + M - 1)sin(\theta_1) \tag{2.34}$$

$$m_2(\theta_2) = (m_{20} + M - 1)cos(\theta_2) + j_{20}sin(\theta_2) + (1 - M) \tag{2.35}$$

$$j_2(\theta_2) = j_{20}cos(\theta_2) - (m_{20} + M - 1)sin(\theta_2) \tag{2.36}$$

The solutions for time interval P2($\alpha_1 < \theta_1 < \gamma_1$):

$$m_1(\theta_1) = (m_{11} - M - 1)cos(\theta_1 - \alpha_1) + j_{11}sin(\theta_1 - \alpha_1) + (1 + M) \tag{2.37}$$

$$j_1(\theta_1) = j_{11}cos(\theta_1 - \alpha_1) - (m_{11} - M - 1)sin(\theta_1 - \alpha_1) \tag{2.38}$$

$$m_2(\theta_2) = (m_{21} - M - 1)cos(\theta_2 - \alpha_2) + j_{21}sin(\theta_2 - \alpha_2) + (1 + M) \tag{2.39}$$

$$j_2(\theta_2) = j_{21}cos(\theta_2 - \alpha_2) - (m_{21} - M - 1)sin(\theta_2 - \alpha_2) \tag{2.40}$$

where m_{10},j_{10},m_{20} and j_{20} are the initial values of m_1,j_1,m_2 and j_2 respectively and m_{11},j_{11},m_{21} and j_{21} are the values of m_1,j_1,m_2 and j_2 respectively at the end of interval P1.

$$\alpha_1 = \omega_{B1}t_1 \tag{2.41}$$

$$\alpha_2 = \omega_{B2}t_1 \tag{2.42}$$

t_1 is the time when the current i_{L1} changes its sign.

State variables at the end of interval P1 are given by eq. 2.37- 2.40.

$$m_{11} = (m_{10} + M - 1)cos(\alpha_1) + j_{10}sin(\alpha_1) + (1 - M) \tag{2.43}$$

$$j_{11} = j_{10}cos(\alpha_1) - (m_{10} + M - 1)sin(\alpha_1) \tag{2.44}$$

$$m_{21} = (m_{20} + M - 1)cos(\alpha_2) + j_{20}sin(\alpha_2) + (1 - M) \tag{2.45}$$

$$j_{21} = j_{20}cos(\alpha_2) - (m_{20} + M - 1)sin(\alpha_2) \tag{2.46}$$

Because of the half-cycle stability and half-cycle odd symmetry of the switching waveforms the state variables at the end of the half-cycle should be the same with opposite sign hence the initial conditions can be given by eq. 2.47- 2.50.

$$-m_{10} = (m_{11} - M - 1)cos(\gamma_1 - \alpha_1) + j_{11}sin(\gamma_1 - \alpha_1) + (1 + M) \tag{2.47}$$

$$-j_{10} = j_{11}cos(\gamma_1 - \alpha_1) - (m_{10} - M - 1)sin(\gamma_1 - \alpha_1) \tag{2.48}$$

$$-m_{20} = (m_{20} - M - 1)cos(\gamma_2 - \alpha_2) + j_{20}sin(\gamma_2 - \alpha_2) + (1 + M) \tag{2.49}$$

$$-j_{20} = j_{20}cos(\gamma_2 - \alpha_2) - (m_{20} - M - 1)sin(\gamma_2 - \alpha_2) \tag{2.50}$$

where

$$\gamma_1 = \frac{\pi}{F_1} \tag{2.51}$$

$$\gamma_2 = \frac{\pi}{F_2} \tag{2.52}$$

where F_1 and F_2 are normalised switching frequencies with ω_{B1} and ω_{B2} respectively.

Substituting the values of initial conditions given by the eq. 2.47- 2.50 into the eq. 2.43- 2.46 the values of j_{11},m_{11},j_{21} and m_{21} can be found in terms of γ_1,α_1 and γ_2 and α_2 respectively as given by eq.

$$j_{11} = B_{i3} + B_{11}cos\,(\alpha_1) + B_{12}sin\,(\alpha_1) \tag{2.53}$$

$$j_{21} = B_{23} + B_{21}cos\,(\alpha_1) + B_{22}sin\,(\alpha_1) \tag{2.54}$$

$$m_{11} = -2\frac{sin\left(\frac{\alpha_1}{2}\right)sin\left(\frac{\gamma_1-\alpha_1}{2}\right)}{cos\left(\frac{\gamma_1}{2}\right)} \tag{2.55}$$

$$m_{21} = -2\frac{sin\left(\frac{\alpha_2}{2}\right)sin\left(\frac{\gamma_2-\alpha_2}{2}\right)}{cos\left(\frac{\gamma_2}{2}\right)} \tag{2.56}$$

At time t_1 the $i_{L1}(t_1) = 0$ and hence reverse transforming the variables j_{11} and j_{21} and solving for α_1 iteratively we can find the value of α_1 and α_2 as following.

$$i_{L1} = \frac{(K_4 i_1 - K_3 i_2)}{(K_4 - K_3)} \tag{2.57}$$

$$j_{L11} = \frac{\left(K_4 j_1 - \frac{K_3}{\omega_{21}} j_2\right)}{(K_4 - K_3)} \tag{2.58}$$

At $t = t_1$ the value of j_{L11} will be given by eq. 2.59.

$$j_{L11}(t_1) = \frac{\left[K_4 \{B_{11}cos(\alpha_1) + B_{12}sin(\alpha_1) + B_{13}\} - \frac{K_3}{\omega_{21}} \{B_{21}cos(\alpha_2) + B_{22}sin(\alpha_2) + B_{13}\}\right]}{(K_4 - K_3)} \tag{2.59}$$

Where B_{11}-B_{23} are defined as given by eq. 2.60- ??.

$$B_{11} = -tan\left(\frac{\gamma_1}{2}\right) \tag{2.60}$$

$$B_{12} = B_{22} = 1 \tag{2.61}$$

$$B_{13} = -Mtan\left(\frac{\gamma_1}{2}\right) \tag{2.62}$$

$$B_{21} = -tan\left(\frac{\gamma_2}{2}\right) \tag{2.63}$$

$$B_{23} = -Mtan\left(\frac{\gamma_2}{2}\right). \tag{2.64}$$

Hence we obtain the following key equation for calculating the value of α_1 and hence α_2 given by eq. 2.65.

$$K_4 (B_{11}cos(\alpha_1) + B_{12}sin(\alpha_1) + B_{13}) - \frac{K_3}{\omega_{12}} (B_{21}cos(\alpha_2) + B_{22}sin(\alpha_2) + B_{13}) = 0 \tag{2.65}$$

The eq. 2.65 can be solved iteratively for given values of a,b,γ_1 and M .

2.2.1.3 Output Characterstics of the Converter

The output characterstics of the converter are the curves between normalised output voltage M and normalised output current J_{o1} at different frequencies. These characterstics can be obtained once the value of M is computed.

$$J_{o1} = \frac{2}{\gamma_1 (K_4 - K_3)} \left\{ K_3 \omega_{12}^2 m_{21} - K_4 m_{11} \right\} \tag{2.66}$$

The output characterstics of the converter given by topology 6 are shown in fig. 2.7-2.9.

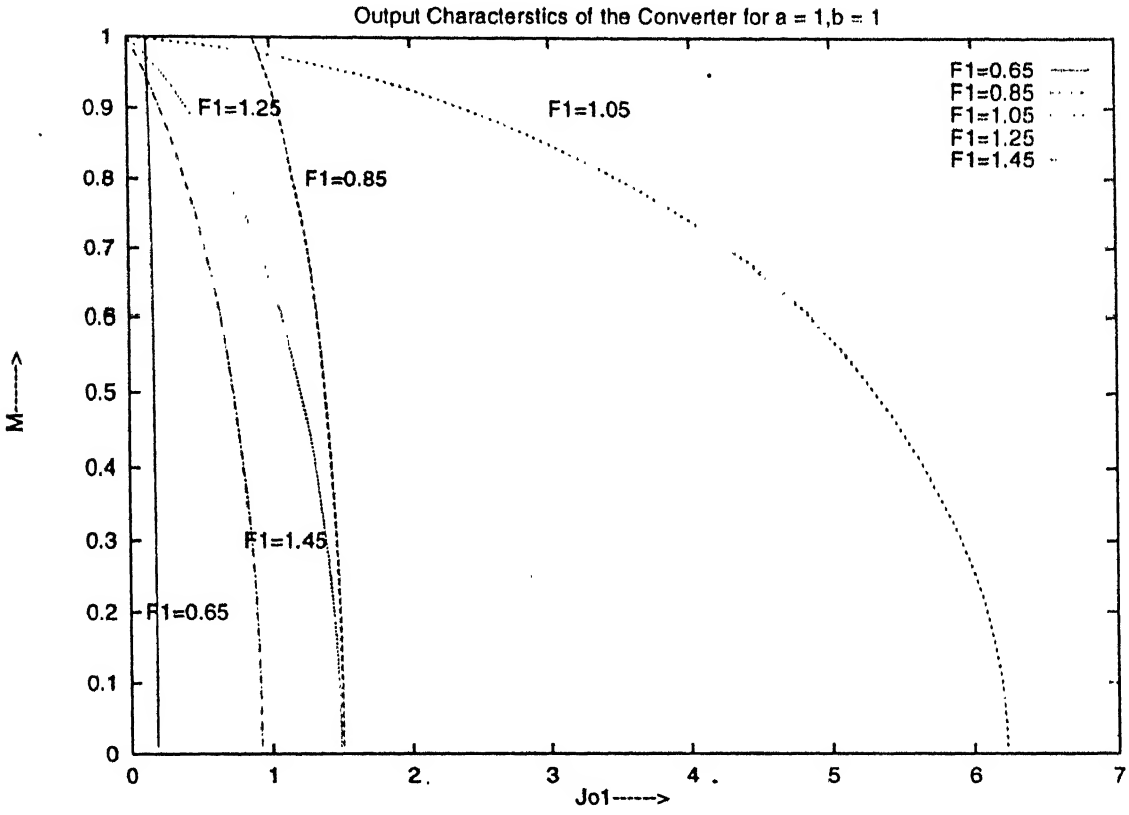

Figure 2.7: Output Characterstics Curves of the converter of topology 6(a = 1,b = 1).

Similar characterstics for $F1 = 0.9$ and for varying values of a and b are shown in fig. 2.10.

The output characterstics obtained by simulation of the converter are shown alongwith the analysis characterstics for $F_1 = 0.92$ in fig. 2.11 and are found to be almost matching. This validates the results of the analysis by the method suggested in this chapter.

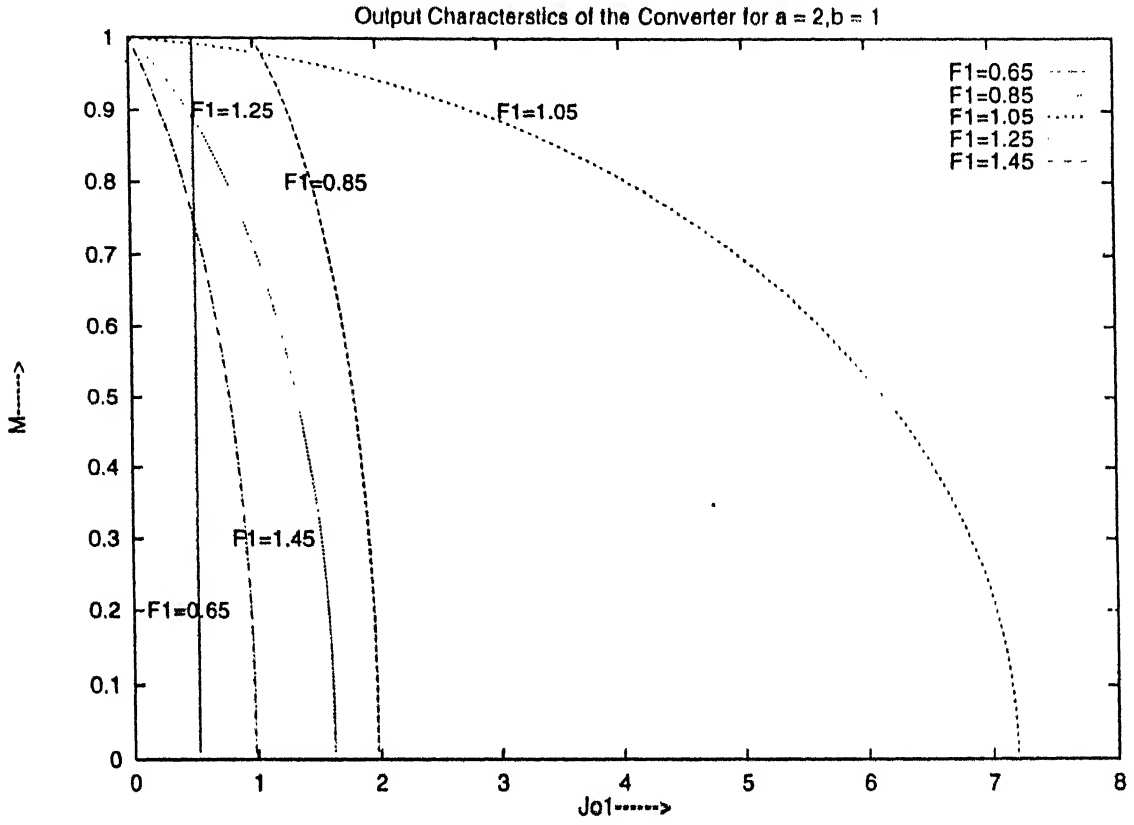

Figure 2.8: Output Characterstics Curves of the converter of topology 6(a = 2,b = 1) for different values of frequencies.

2.2.1.4 Gain of the Converter

The DC gain of the converter is one of the most important parameters and can be determined as following.

The average inverter current current is given by eq. 2.67.

$$I_{in} = \frac{2}{T_s}\int_0^{\frac{T_s}{2}} i_{L1}(t)dt \tag{2.67}$$

putting $i_{L1}(t)$ in terms of i_1 and i_2 as given by eq. 2.68- 2.72 and using the decoupled state equations of eq. 2.15- 2.18 the normalised average inverter output current is given by eq. 2.72.

$$i_{L1} = \frac{(K_4 i_1 - K_3 i_2)}{(K_4 - K_3)} \tag{2.68}$$

$$i_{L2} = \frac{(i_1 - i_2)}{(K_3 - K_4)} \tag{2.69}$$

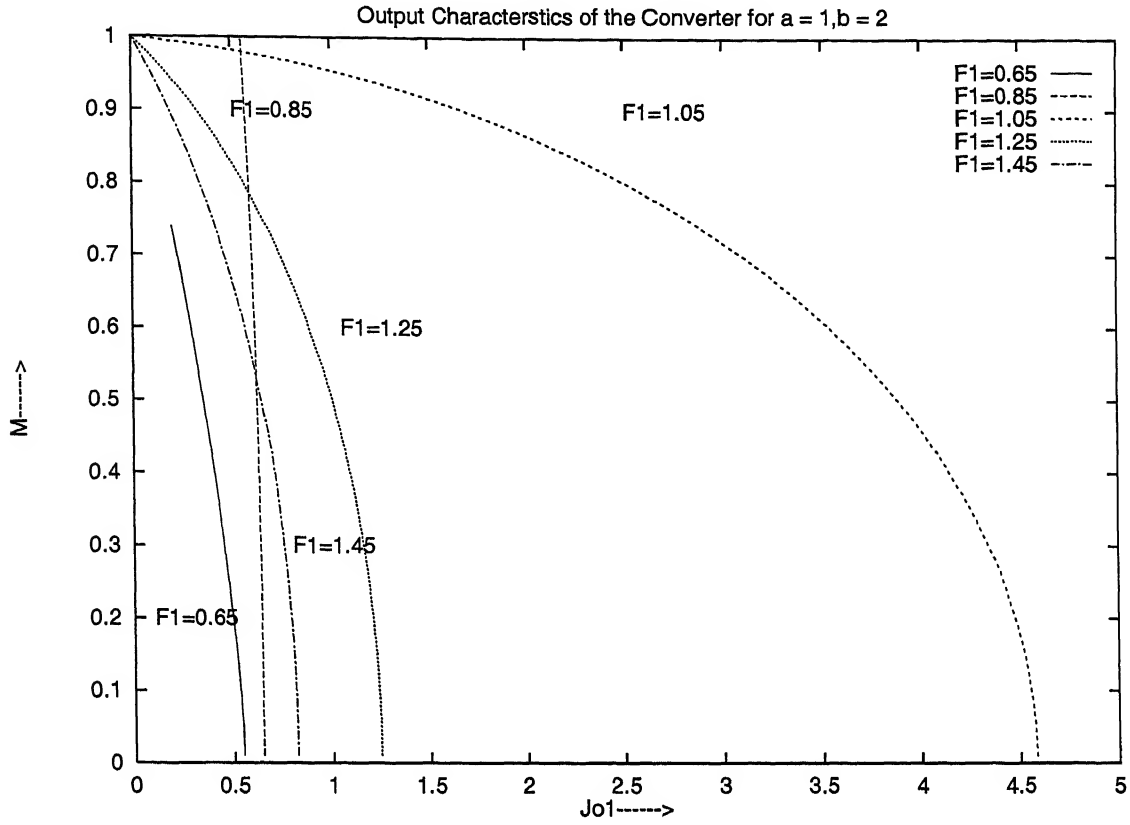

Figure 2.9: Output Characterstics Curves of the converter of topology 8(a = 1,b = 2).

$$v_{C1} = \frac{(K_2 v_1 - K_1 v_2)}{(K_2 - K_1)} \tag{2.70}$$

$$v_{C2} = \frac{(v_1 - v_2)}{(K_1 - K_2)} \tag{2.71}$$

$$J_{in1} = abs\left(\frac{2}{\gamma_1}\frac{(K_1 + a)}{a}\frac{(K_2 m_{10} - K_1 m_{20})}{(K_2 - K_1)}\right) \tag{2.72}$$

Applying power balance to the input and output of the converter we have:

$$V_s I_{in} = V_o I_o \tag{2.73}$$

We also have relation between output current and output voltage and load (Q_{p1}) defined by eq. 2.74.

$$J_{o1} = Q_{p1} M \tag{2.74}$$

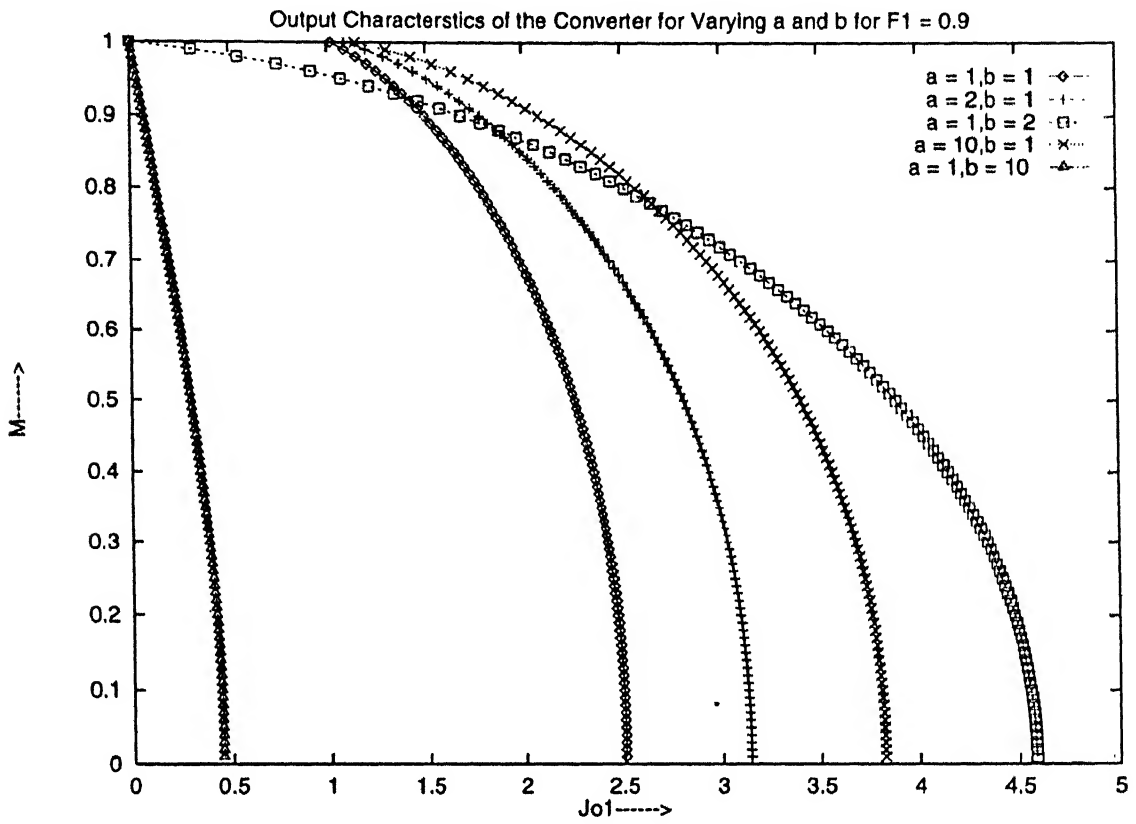

Figure 2.10: Output Characterstics Curves of the converter of topology 6 (F1 = 0.9 with a and b varied.

From eq. 2.18- 2.21 we can find the following relation:

$$M = \sqrt{\frac{J_{in1}}{Q_{p1}}} \tag{2.75}$$

where Q_{p1} is defined as:

$$Q_{p1} = \frac{\sqrt{\frac{L1}{C11}}}{R_L} \tag{2.76}$$

Solving eq. 2.72- 2.76 iteratively we can find the value of converter gain and α_1 simultaneously for given value of F_1 and Q_{p1}.

The converter gain curves are drawn based on the above discussion for different values of a,b and Q_{p1} and are shown in fig. 2.12- 2.14

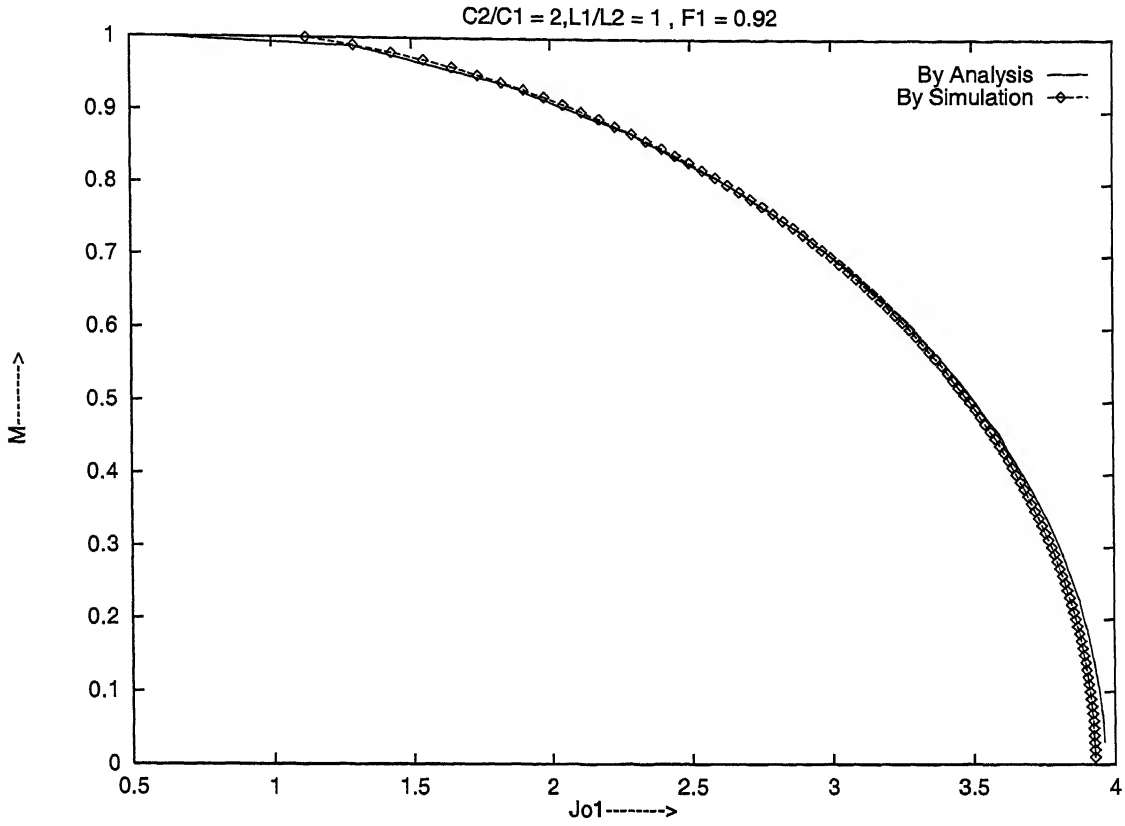

Figure 2.11: Output characterstics by Simulation and analysis for $a = 2, b = 1$ and $F_1 = 0.92$.

2.2.2 Complex Circuit Analysis Technique

This technique is based on the assumption- that most of the energy supplied by the source is at the fundamental frequency. Hence it is possible to replace the square-wave voltage source by a sinusoidal voltage source(see fig. 2.15). Moreover , to account for the effect of bridge rectifier the load resistance is replaced by an equivalent resistance R_{ac} which is calculated as suggested in the following section.

2.2.3 Effect of Bridge Rectifier on the Value of Load Resistance

In fig. 2.16 I_b and V_b represent the rms fundamental components of i_b(t) and v_b(t) respectively. Because of the diode bridge rectifier and the capacitive filter (C_O) present in the output circuit, the DC output current is obtained as the average of

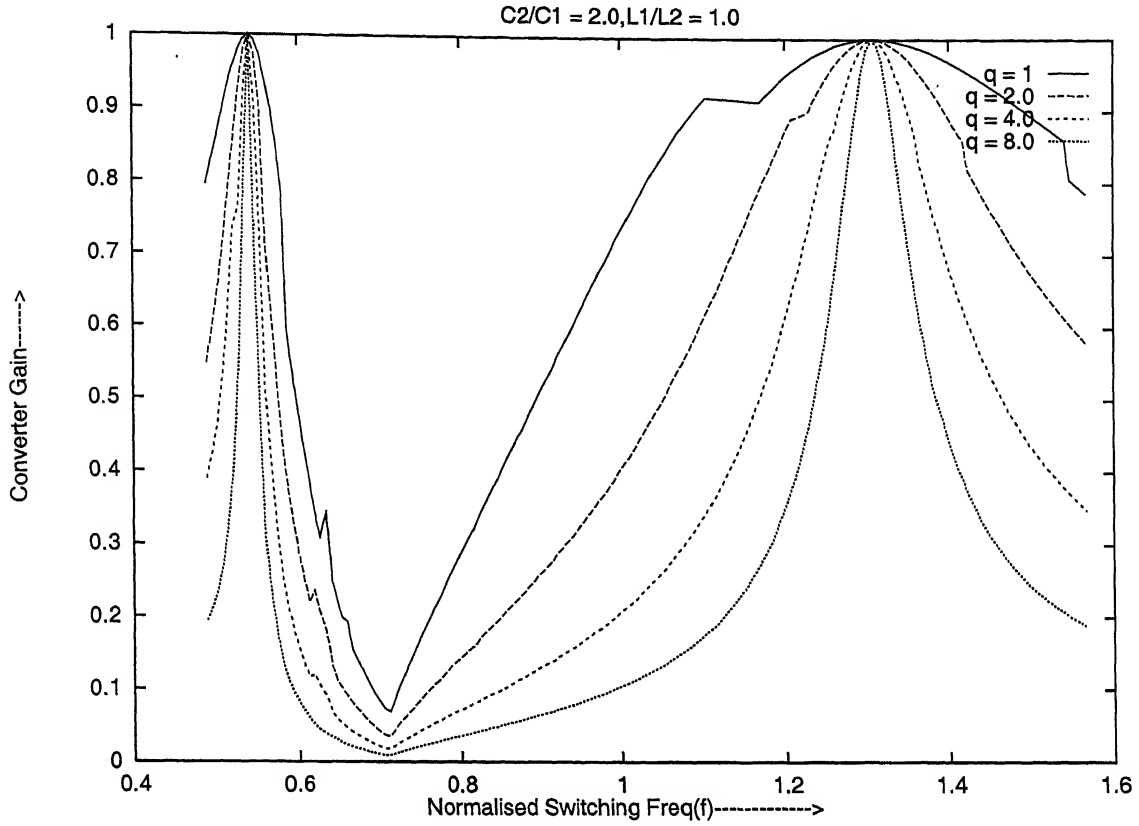

Figure 2.12: Gain vs Frequency Curves for $a = 2$ and $b = 1$ Using Time Domain Analysis.

input ac current,i_b(t),

$$I_o = \frac{1}{\pi}\int_0^{\pi} \sqrt{2} I_b sin(\omega t) d(\omega t) \tag{2.77}$$

where $\omega = 2\pi$f and f is the switching frequency

$$I_o = \frac{2\sqrt{2}}{\pi} I_b \tag{2.78}$$

The fundamental component of the diode bridge voltage (output voltage reflected to bridge input) is calculated from Fourier analysis.

$$V_b = \frac{1}{\sqrt{2\pi}}\int_0^{2\pi} v_b(t) sin(\omega t) d(\omega t) \tag{2.79}$$

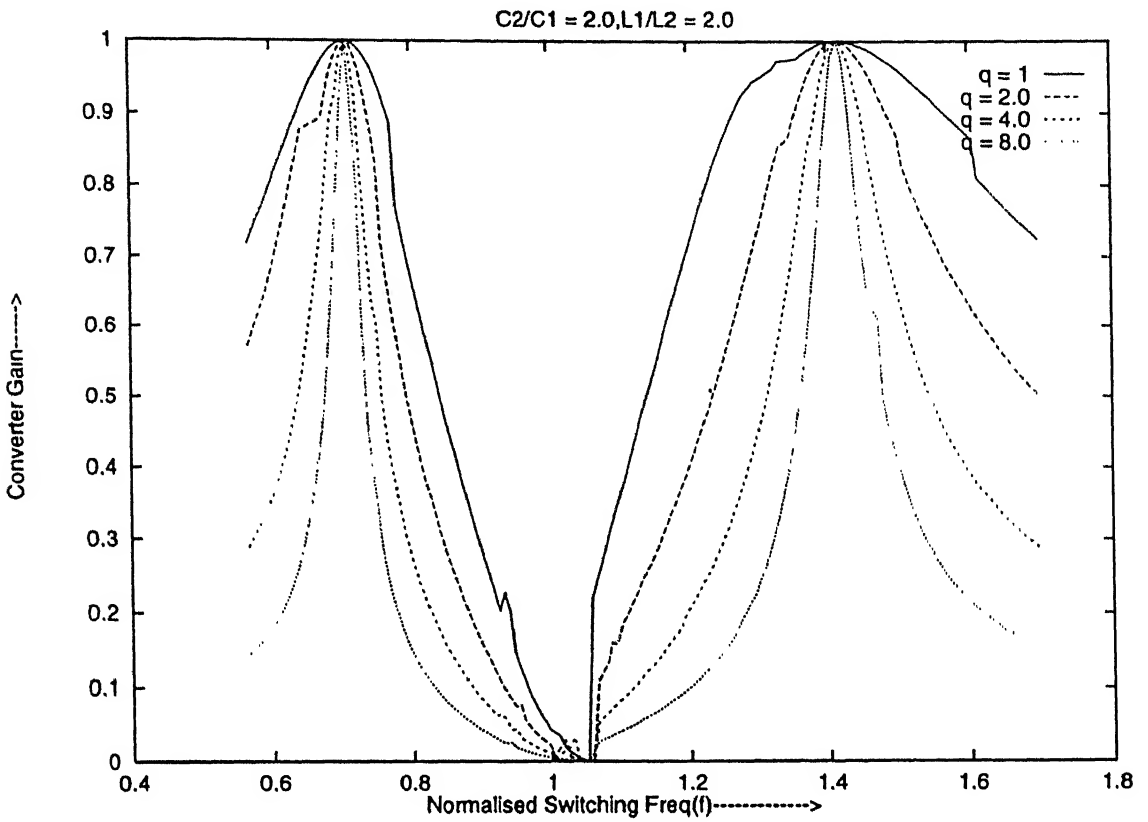

Figure 2.13: Gain vs Frequency Curves for $a = 2$ and $b = 2$ Using Time Domain Analysis.

$$V_b = \frac{2\sqrt{2}}{\pi} V_o \tag{2.80}$$

Using eq. 2.78 and 2.80,equivalent ac resistance is given by

$$R_{ac} = \frac{V_b}{I_b} = \frac{8}{\pi^2} \frac{V_o}{I_o} \tag{2.81}$$

$$R_{ac} = \frac{8}{\pi^2} R_L \tag{2.82}$$

where $R_L = \frac{V_o}{I_o}$.

2.2.4 Description Of the Technique

The rms fundamental component of the inverter output voltage at terminals AB (see fig. 2.15) can be found using the waveform shown in fig. 2.17. The duty ratio,D is

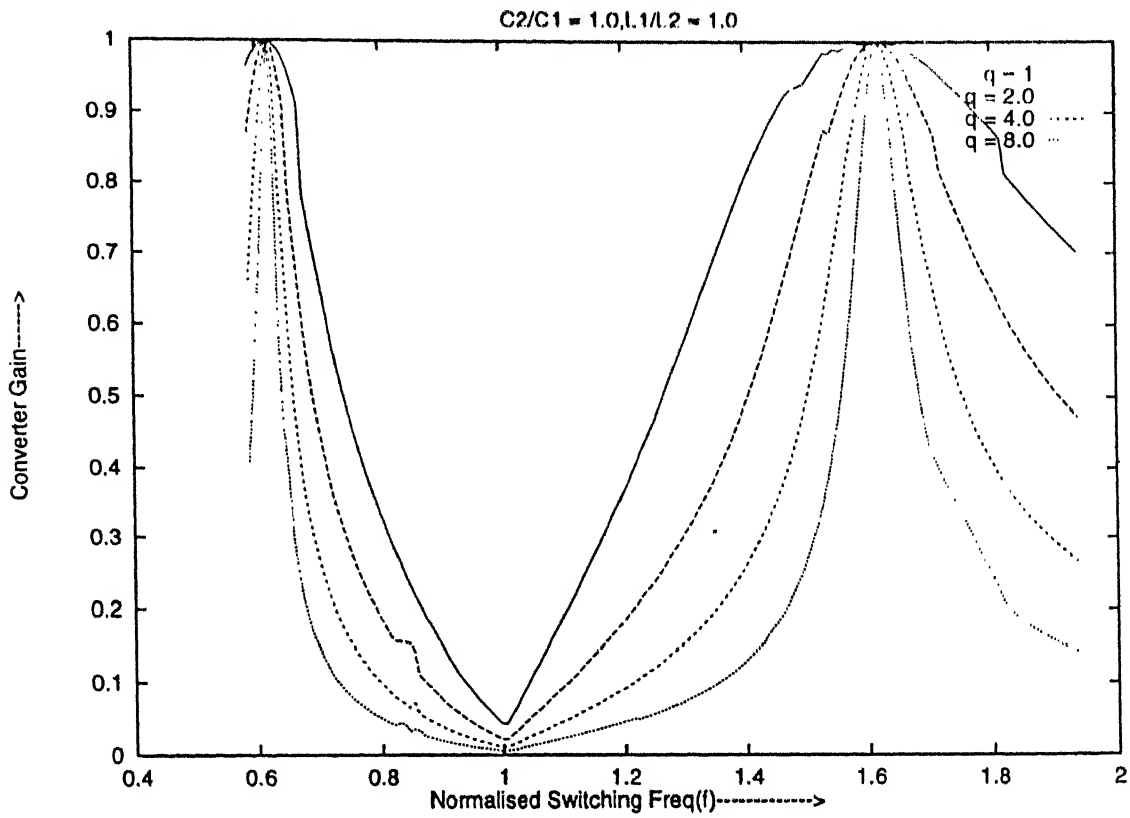

Figure 2.14: Gain vs Frequency Curves for $a = 1$ and $b = 1$ Using Time Domain Analysis.

defined as the ratio of the time duration for which S1 and S2 or S3 and S4 are switched on simultaneously (T_{on}) to the half of the switching period($\frac{T_s}{2}$),

$$D = \frac{T_{on}}{\frac{T_s}{2}} \tag{2.83}$$

we define a new angular variable δ by eq. 2.84.

$$\delta = \pi D \tag{2.84}$$

The rms fundamental voltage

$$V_{AB} = \frac{1}{\sqrt{2}} \cdot \frac{1}{\pi} \int_0^{2\pi} v_{AB}(t) sin(\omega t) d(\omega t) \tag{2.85}$$

$$V_{AB} = \frac{1}{\sqrt{2}} \cdot \frac{1}{\pi} \left\{ \int_{\frac{\pi-\delta}{2}}^{\frac{\pi+\delta}{2}} V_g sin(\omega t) d(\omega t) - \int_{\frac{3\pi-\delta}{2}}^{\frac{3\pi+\delta}{2}} V_g sin(\omega t) d(\omega t) = \frac{2\sqrt{2}}{\pi} V_g sin(\frac{\delta}{2}) \right\} \tag{2.86}$$

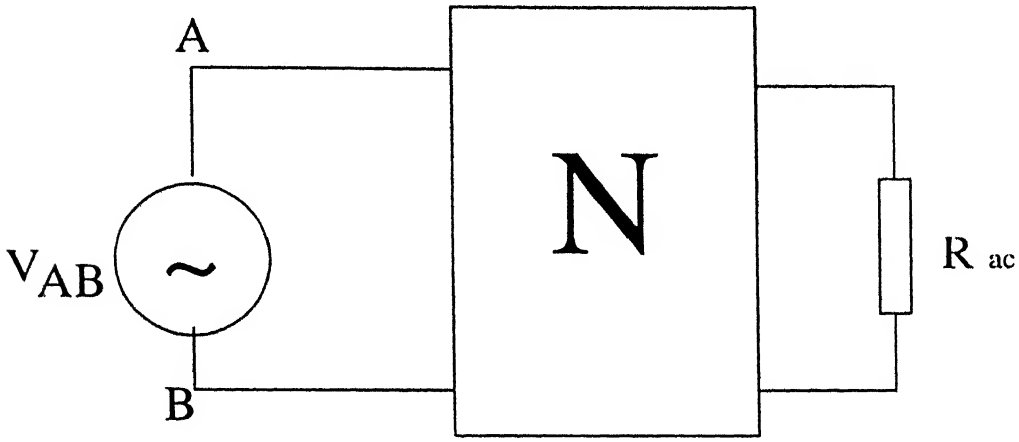

N - nth order resonant tank network.
R_{ac} - AC equivalent load resistance.
V_{AB} - rms fundamental component of $V_{AB}(t)$.

Figure 2.15: AC equivalent circuit of general resonant converter

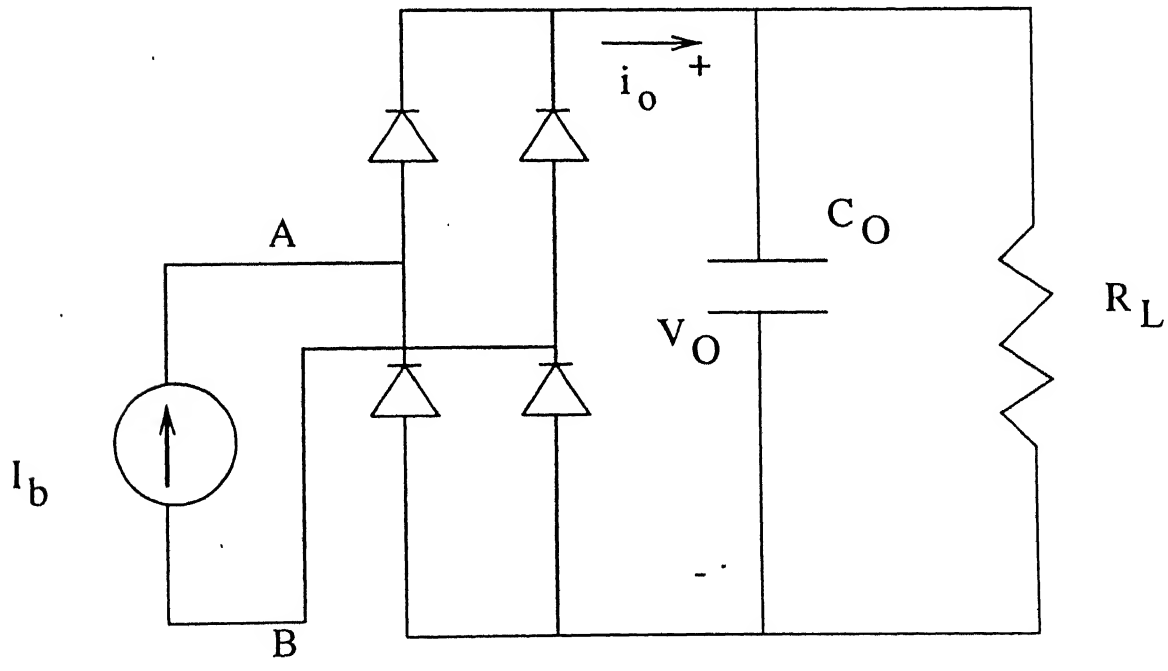

Figure 2.16: Circuit diagram of output bridge rectifier and filter

The generalised AC equivalent circuit of the resonant converter is shown in fig 2.15.

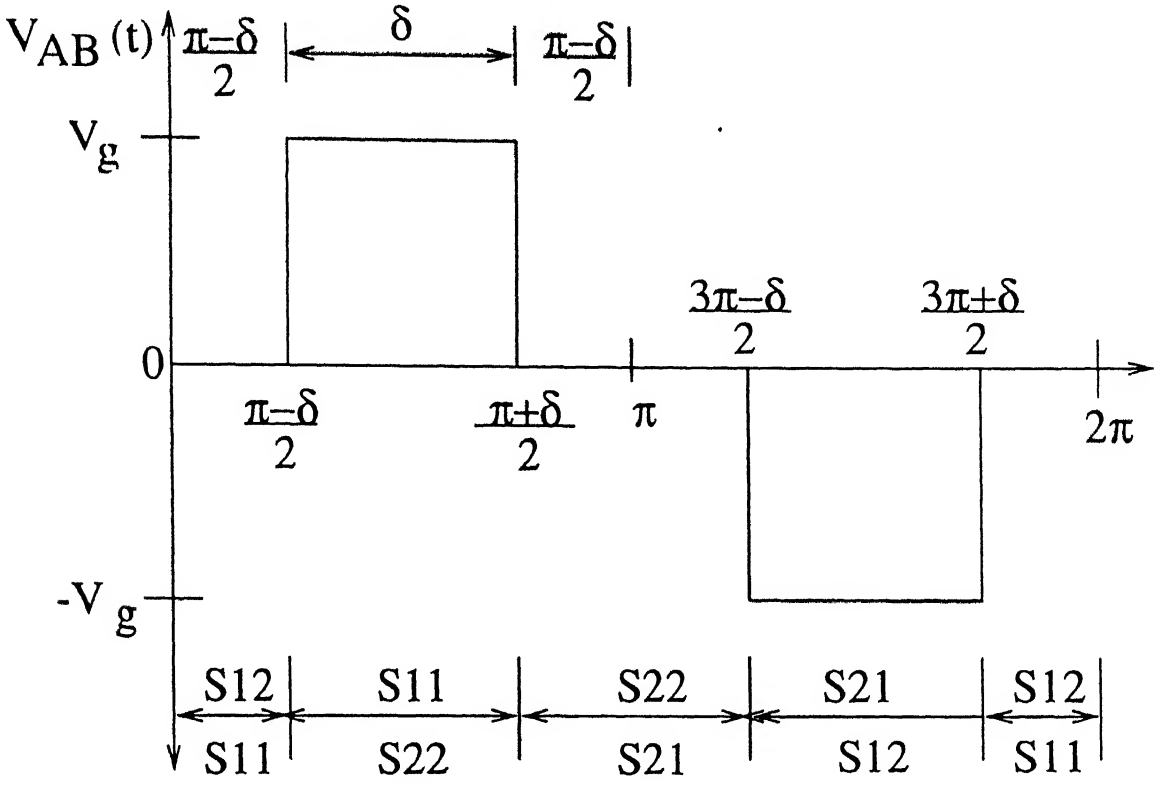

Figure 2.17: The wave form of the inverter output voltage $v_{AB}(t)$.

In this section topology 8 is taken for describing the details of the technique. The equivalent circuit of topology 8 is shown in fig. 2.18. The gain of the converter which

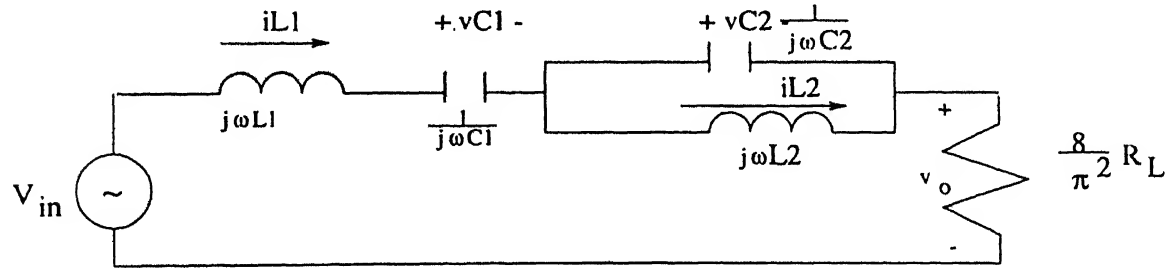

Figure 2.18: AC equivalent circuit of topology 8.

is defined by eq. 2.87 can be calculated by simple AC circuit analysis.

$$M = \frac{V_o}{V_s} \tag{2.87}$$

hence

$$M = \frac{8}{\pi^2} \frac{R_L}{|Z1 + Z2|} \tag{2.88}$$

where

$$Z1 = \frac{1-\omega^2 L1C1}{j\omega C1} \tag{2.89}$$

and

$$Z2 = \frac{8}{\pi^2}R_L + \frac{j\omega L2}{1-\omega^2 L2C2} \tag{2.90}$$

By using eqns. 2.87- 2.90 and using the normalised variables as defined in Appendix-A the gain of the converter can be given by eq. 2.91.

$$M = \frac{1}{1 - j\frac{\pi^2 Q_1}{8}\left\{\frac{\frac{a}{b}\omega_n{}^4 - \left(1+\frac{a}{b}+\frac{1}{b}\right)\omega_n^2+1}{\omega_n\left(1-\frac{a}{b}\omega_n^2\right)}\right\}} \tag{2.91}$$

The gain V_s normalised angular frequency(ω_n) curves are obtained by eq. 2.91 and these are shown in fig. 2.19- 2.20 for different values of a and b whereas similar curves for other topologies are shown in fig. ??- ?? for a=1 and b=1. From eq. 2.91 it is

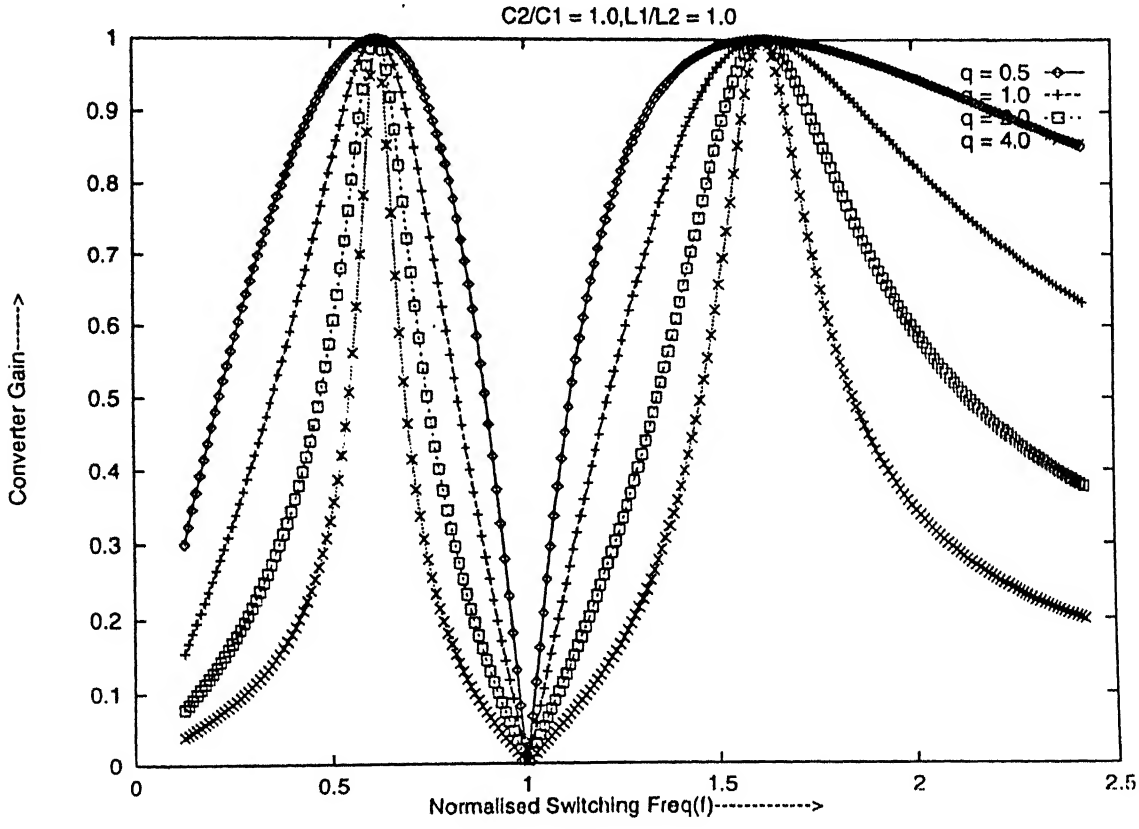

Figure 2.19: Gain vs Normalised Switch Freq. Curves for Various Load Resistaces a=1,b=1

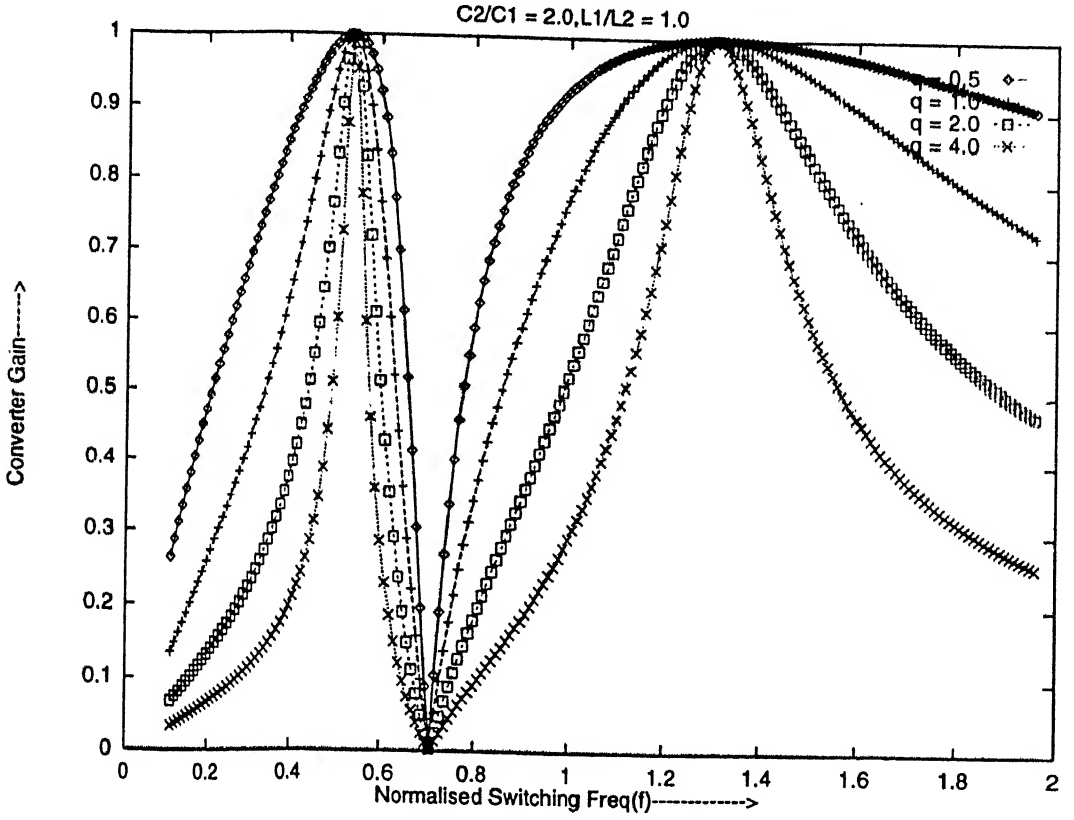

Figure 2.20: Gain vs Normalised Switch Freq. Curves for Various Load Resistaces a=2,b=1

observed that the only term which depends on the load resistance is Q and if the term containing it is zero then the gain of the converter will be independent of the load and will be given by

$$M = sin(\frac{\delta}{2}) \tag{2.92}$$

The converter gain is plotted with respect to duty cycle(D) in fig. 2.21 and the plot found by simulation is matching with that found by eq. 2.92.

2.2.5 Calculation of Component Stresses

From the equivalent circuit the following equations for the component str obtained:

$$j_{L1p} = \frac{4}{\pi |Z_n|}$$

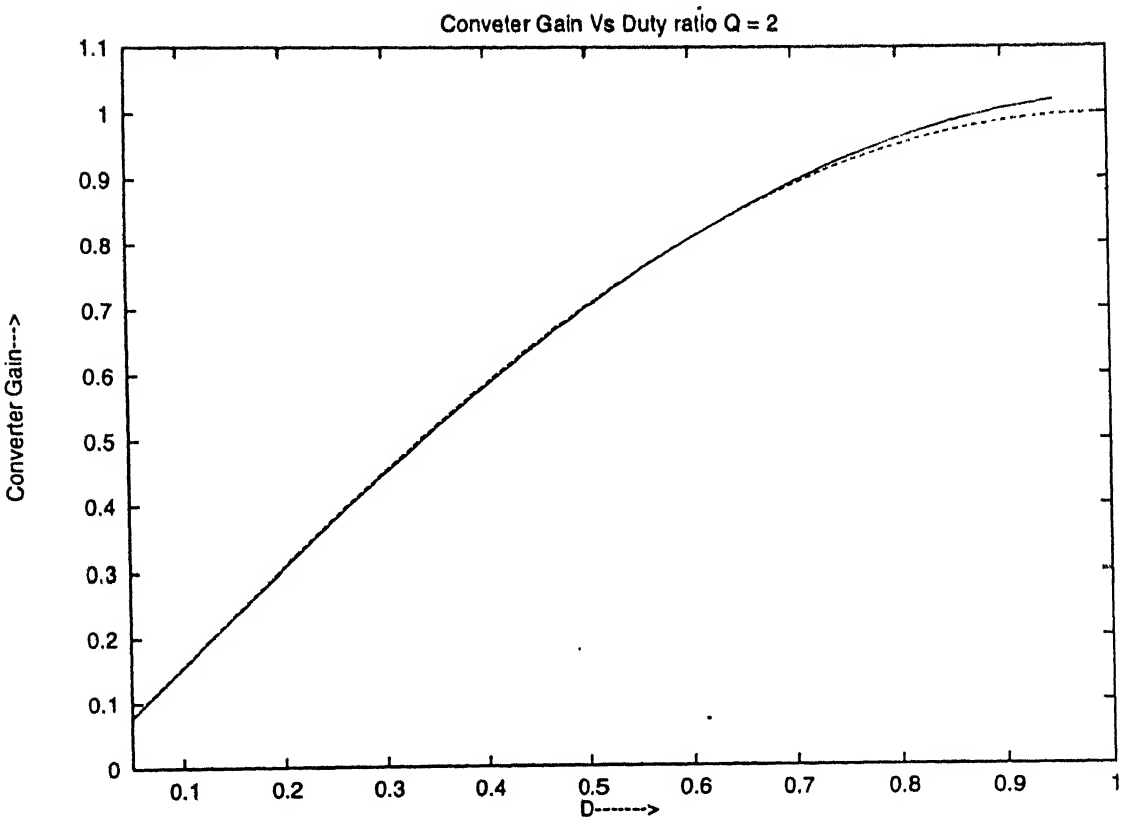

Figure 2.21: Conveter Gain for Varying Duty Ratio (D),$Q_1 = 2$

where Z_n is the normalised input impedence of the network shown in fig. 2.18. hence

$$Z_n = \frac{\left\{\frac{8}{\pi^2}R_L + j\omega L1 + \frac{1}{j\omega C1} + \frac{j\omega L2}{(1-\omega^2 L2C2)}\right\}}{\sqrt{L1C1}} \tag{2.94}$$

$$Z_n = \left\{\frac{8}{\pi^2 Q_1} + j\omega_n + \frac{1}{j\omega_n} + \frac{j\omega_n}{b\left(1 - \frac{a}{b}{\omega_n}^2\right)}\right\} \tag{2.95}$$

$$m_{C1p} = \left|\frac{j_{L1p}}{\omega_n}\right| \tag{2.96}$$

$$m_{C2p} = \left|\frac{j_{L1p}\omega_n}{b\left(1 - \frac{a}{b}\omega_n^2\right)}\right| \tag{2.97}$$

$$j_{L2p} = \left|\frac{j_{L1p}}{\left(1 - \frac{a}{b}\omega_n^2\right)}\right| \tag{2.98}$$

Similarily the stresses of other topologies can be computed by applying simple AC circuit analysis.

The stresses obtained by actual simulation of the converter and those calculated by CCA for different topologies are shown in figures 2.22- 2.27.

From fig. 2.22- 2.27 it is observed that the component stresses calculated by CCA and actual solutions are almost matching for all the topologies if the frequency of operation is ω_{o2}.

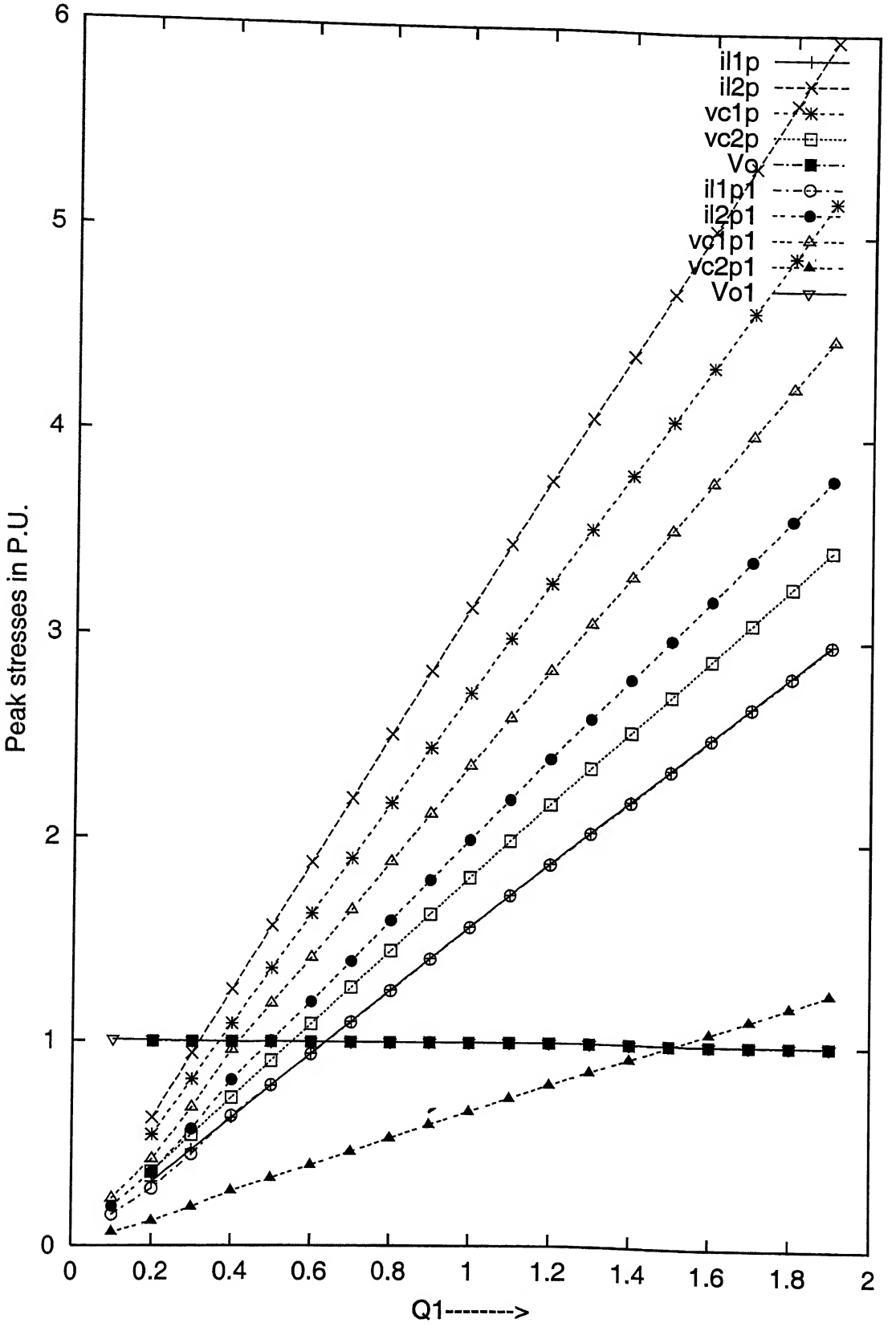

Figure 2.22: Normalised Peak values of different state variables by differential equation method and CCA method(Variables with subscript 1 represent those obtained by actual simulation whereas others are those found by CCA)(Topology 13)

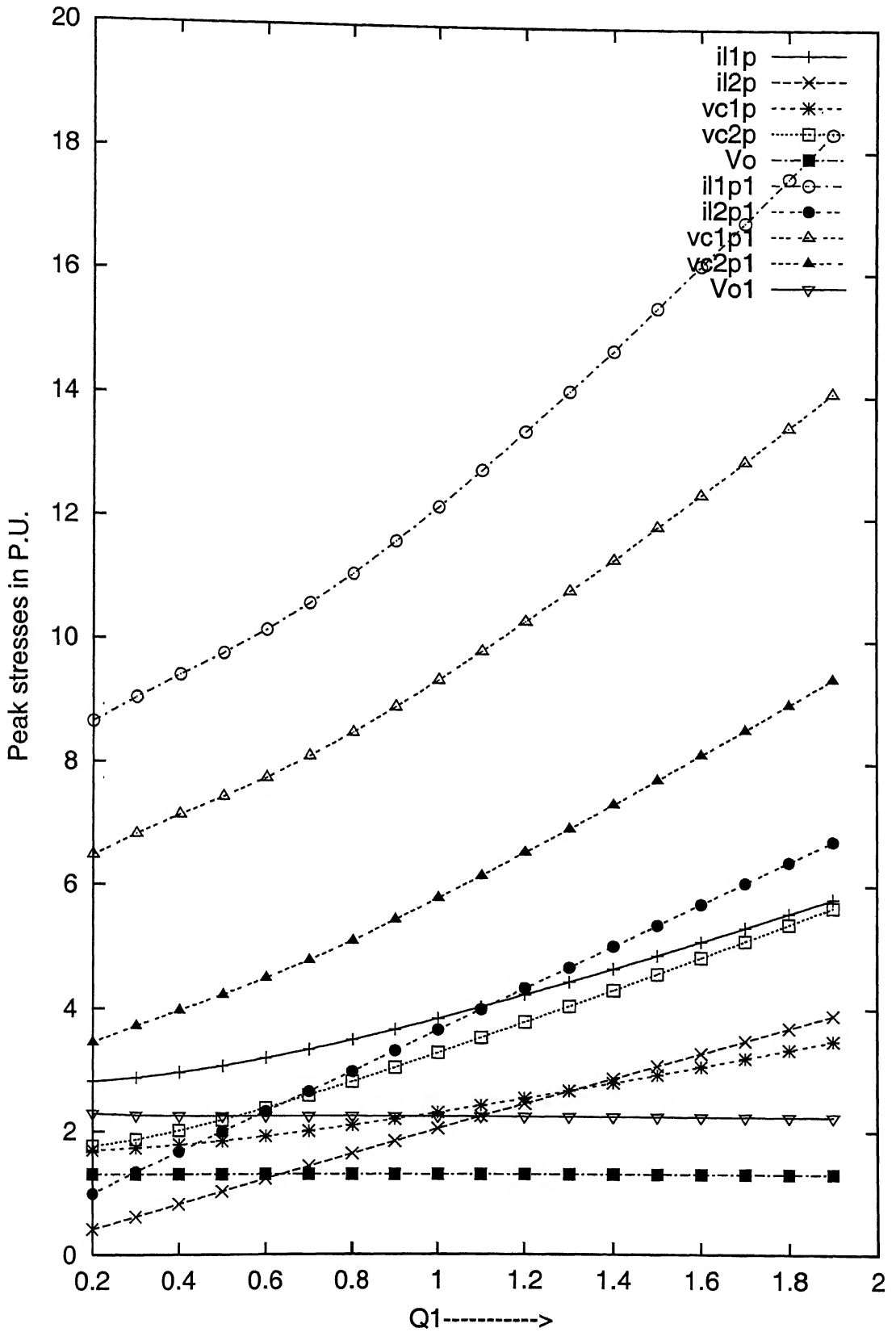

Figure 2.23: Normalised Peak values of different state variables by differential equation method and CCA method(Variables with subscript 1 represent those obtained by actual simulation whereas others are those found by CCA)(Topology 2).

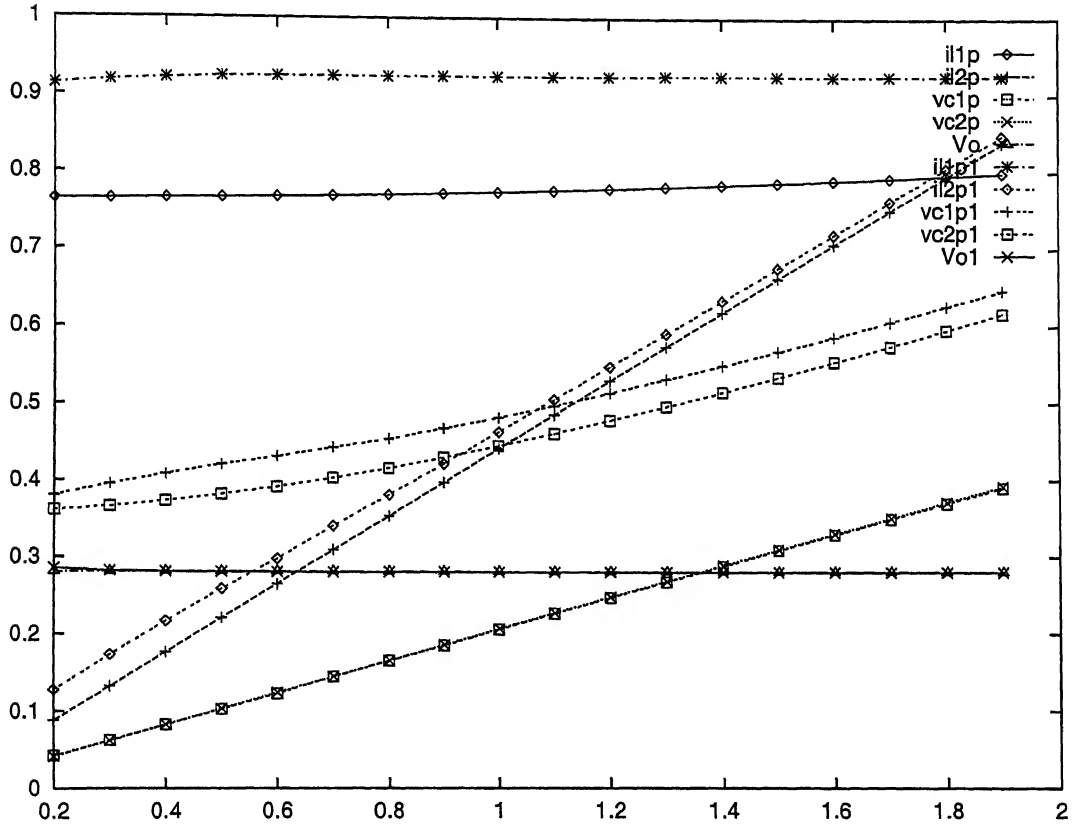

Figure 2.24: Normalised Peak values of different state variables by differential equation method and CCA method(Variables with subscript 1 represent those obtained by actual simulation whereas others are those found by CCA)(Topology 3).

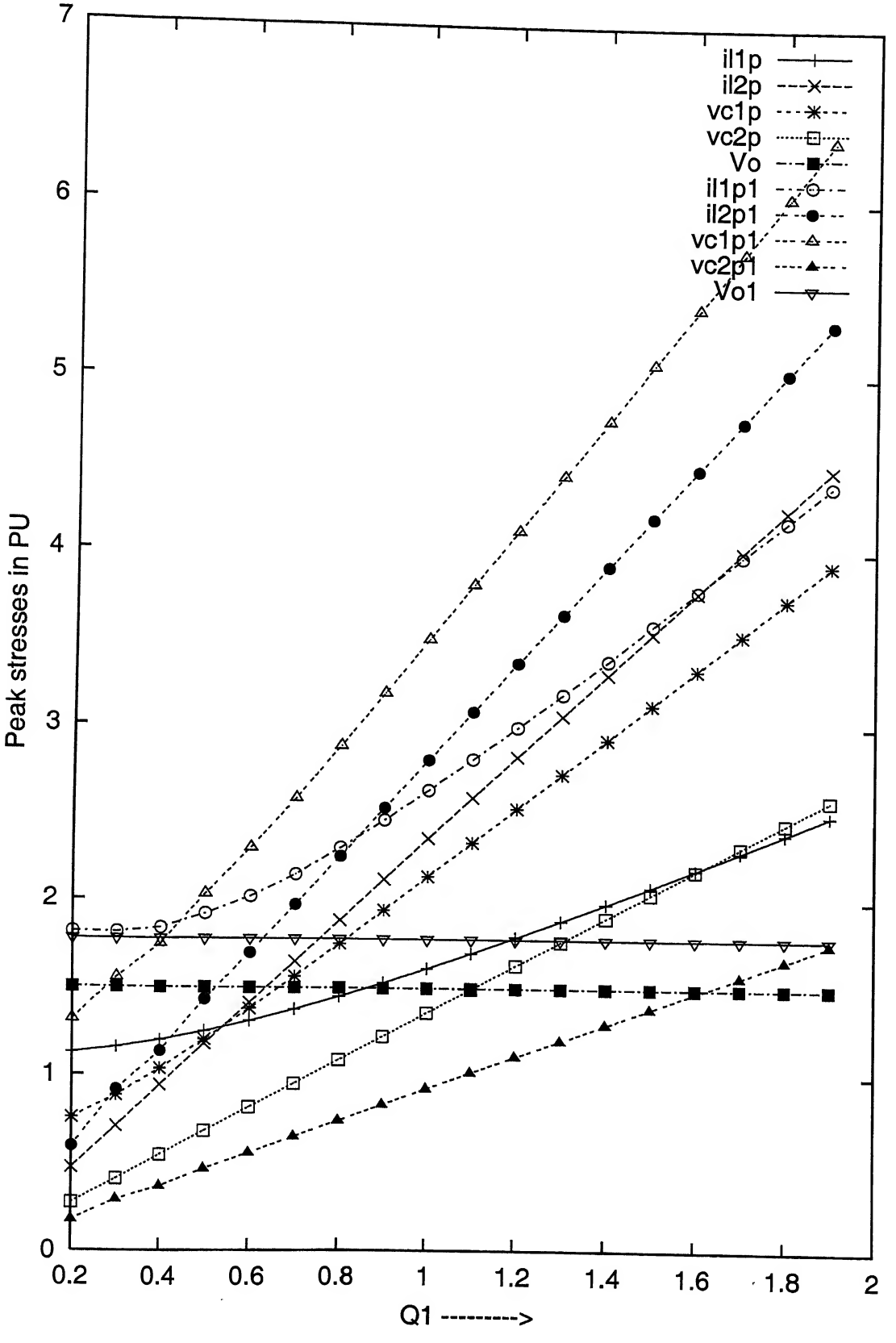

Figure 2.25: Normalised Peak values of different state variables by differential equation method and CCA method(Variables with subscript 1 represent those obtained by actual simulation whereas others are those found by CCA)(Topology 5)

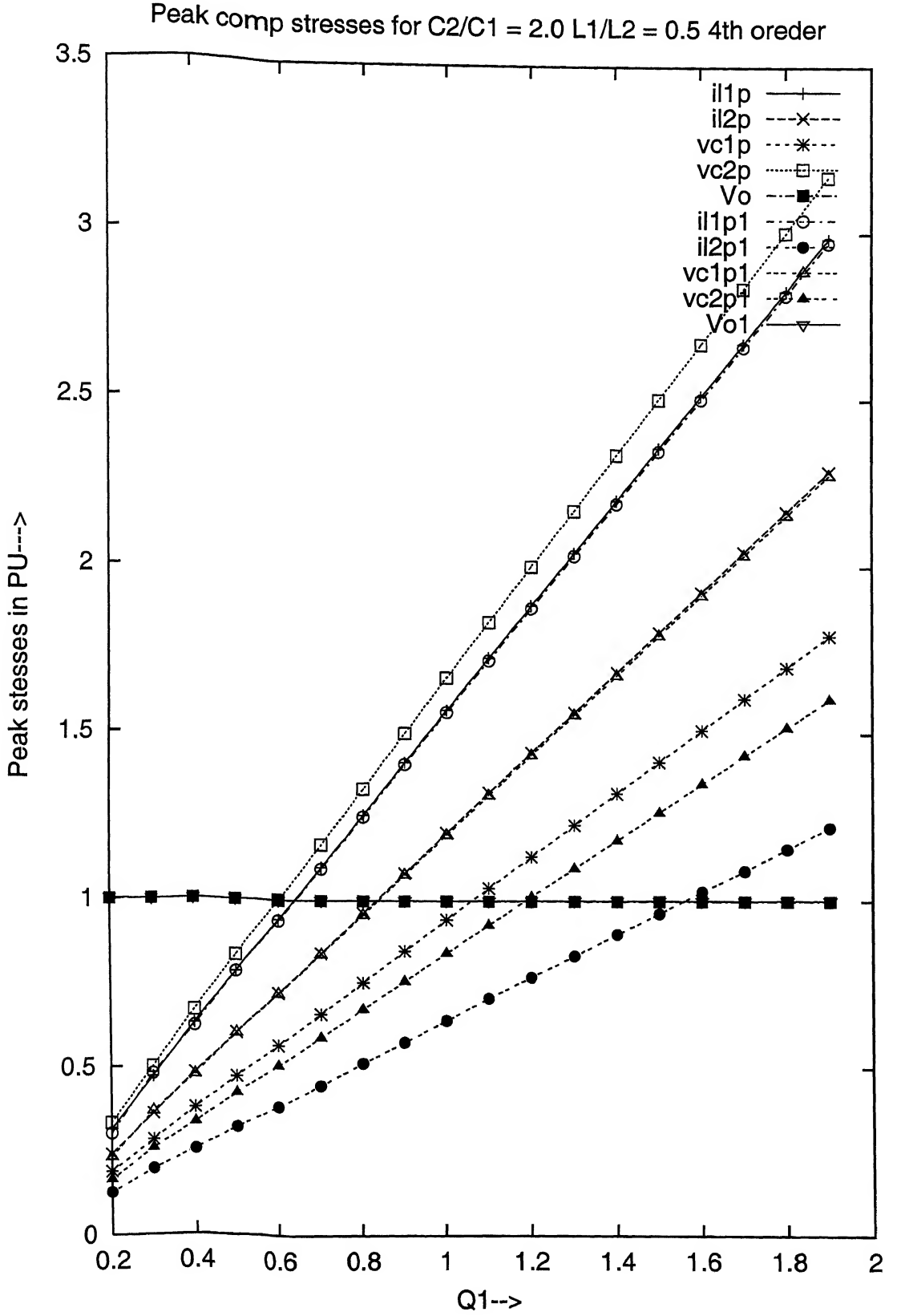

Figure 2.26: Normalised Peak values of different state variables by differential equation method and CCA method(Variables with subscript 1 represent those obtained by actual simulation whereas others are those found by CCA)(Topology 8).

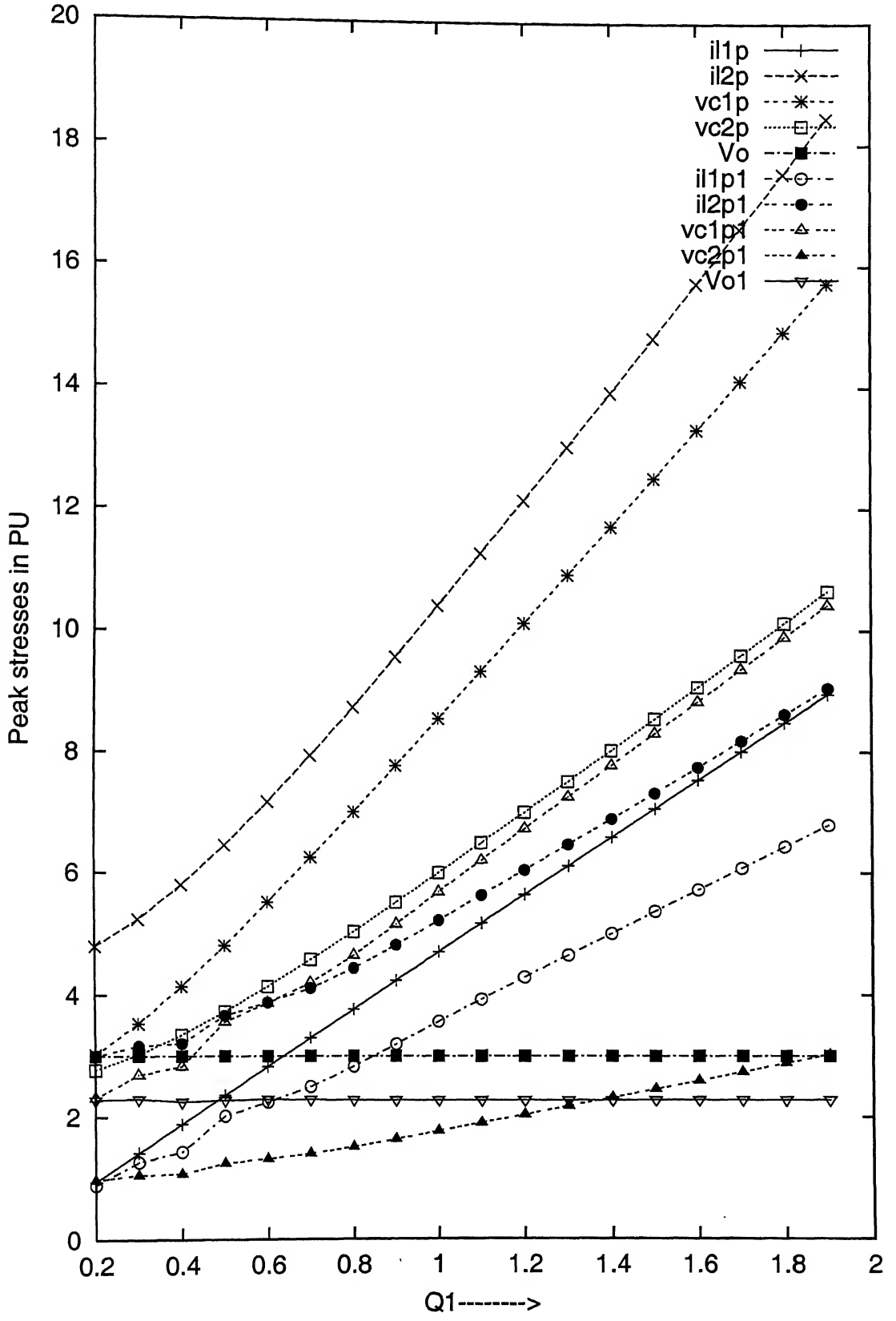

Figure 2.27: Normalised Peak values of different state variables by differential equation method and CCA method(Variables with subscript 1 represent those obtained by actual simulation whereas others are those found by CCA)(Topology 7).

Chapter 3

Selection of Topology

3.1 Introduction

The selection of the suitable topology is one of the most difficult task when the order of the converter increases. There are 98 possible topologies with 4-elements (2 inductors and 2 capacitors) [13]. Out of which 16 are pointed to be of voltage source and voltage sink type. These topologies are listed in fig 2.1. Out of these 16 topologies 4 are just shunt type and they are not considered because in these there is no control of output voltage (which always remains same as that of the input voltage). Out of remaining 12 topologies those topologies are considered in which the leakage inductance of the transformer can be added into one of the resonant inductors . Hence only 6 topologies which are described in appendix-A are used for further study.

3.1.1 Selection Methodology

3.1.1.1 Statement Of The Problem Of Selection Of Appropriate Topology

Given:
4 elements- 2 inductors L_1 & L_2 and 2 capacitors C_1 & C_2 of some value.
Objective:
To select the topology using these four elements,which gives minimum value of the optimising function given by eq. 3.1 for all possible load resistances.

3.1.1.2 Minimum Component Stress Method

Let i_{L1_p},i_{L2_p},v_{C1_p} and v_{C2_p} be the peak current stresses on L_1 & L_2 and peak voltage stresses on C_1 & C_2 respectively. Let v_o be the steady state output voltage of the converter.

The sum of the peak energy stored in each elements of the system will be:

$$S = \frac{1}{2}(C_1 {v_{C1_p}}^2 + C_2 {v_{C2_p}}^2 + L_1 {i_{L1_p}}^2 + L_2 {i_{L2_p}}^2) \tag{3.1}$$

Because this energy will vary as the output load changes so for comparision purpose we should normalise this function by output power.
Let

$$S1 = \frac{2S}{P_o} \tag{3.2}$$

Where

$$P_o = \frac{{v_o}^2}{R_o} \tag{3.3}$$

Hence we get

$$S1 = \frac{j_{L1_p}^2 + \frac{j_{L2_p}^2}{b} + m_{C1_p}^2 + a m_{C2_p}^2}{Q_1 \omega_o M^2} \tag{3.4}$$

j and m repersent the normalised currents and voltages respectively.

The value of $\omega_o = \frac{1}{\sqrt{L_1 C_1}}$ is same for all the converters hence the optimising function can be taken to be

$$S2 = \frac{j_{L1_p}^2 + \frac{j_{L2_p}^2}{b} + m_{C1_p}^2 + a m_{C2_p}^2}{Q_1 M^2} \tag{3.5}$$

3.1.2 Selection of Operating Frequency

One of the objectives of any DC-DC converter is its load independent operation. We have observed in the analysis that if the frequency of operation is either of the ω_{o1} or ω_{o2} as defined by eq. 3.6- 3.7, the output voltage of all the converters remain load independent.

$$\omega_{o1} = \frac{(1 + \frac{L1C1}{L2C2} + \frac{C1}{C2}) - \sqrt{(1 + \frac{L1C1}{L2C2} + \frac{C1}{C2})^2 - 4\frac{L1C1}{L2C2}}}{2} \tag{3.6}$$

$$\omega_{o2} = \frac{(1 + \frac{L1C1}{L2C2} + \frac{C1}{C2}) + \sqrt{(1 + \frac{L1C1}{L2C2} + \frac{C1}{C2})^2 - 4\frac{L1C1}{L2C2}}}{2} \tag{3.7}$$

Hence we select the higher of the two frequencies(ω_{o2}) to be the operating frequency for load independent operation.

3.1.3 Optimisation of the Function

In fig. 3.1- 3.5 the value of the optimising function given by eq. 3.5 vs q is plotted with different ratios *a* and *b* and full duty cycle for all the six topologies to be considered for the selection. From fig. 3.1- 3.4 it is obvious that topology 83 gives the minimum value

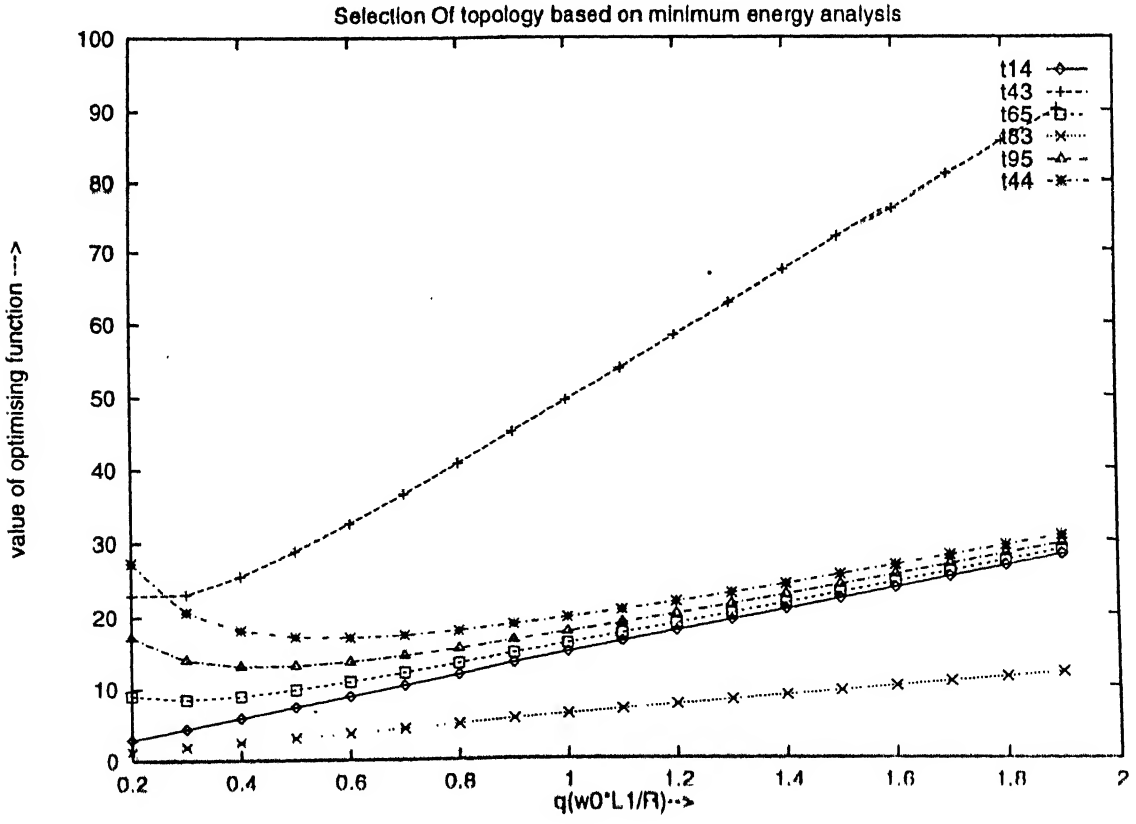

Figure 3.1: Value of Optimising function for different values of q,D = 1, a = 0.5, b = 0.5

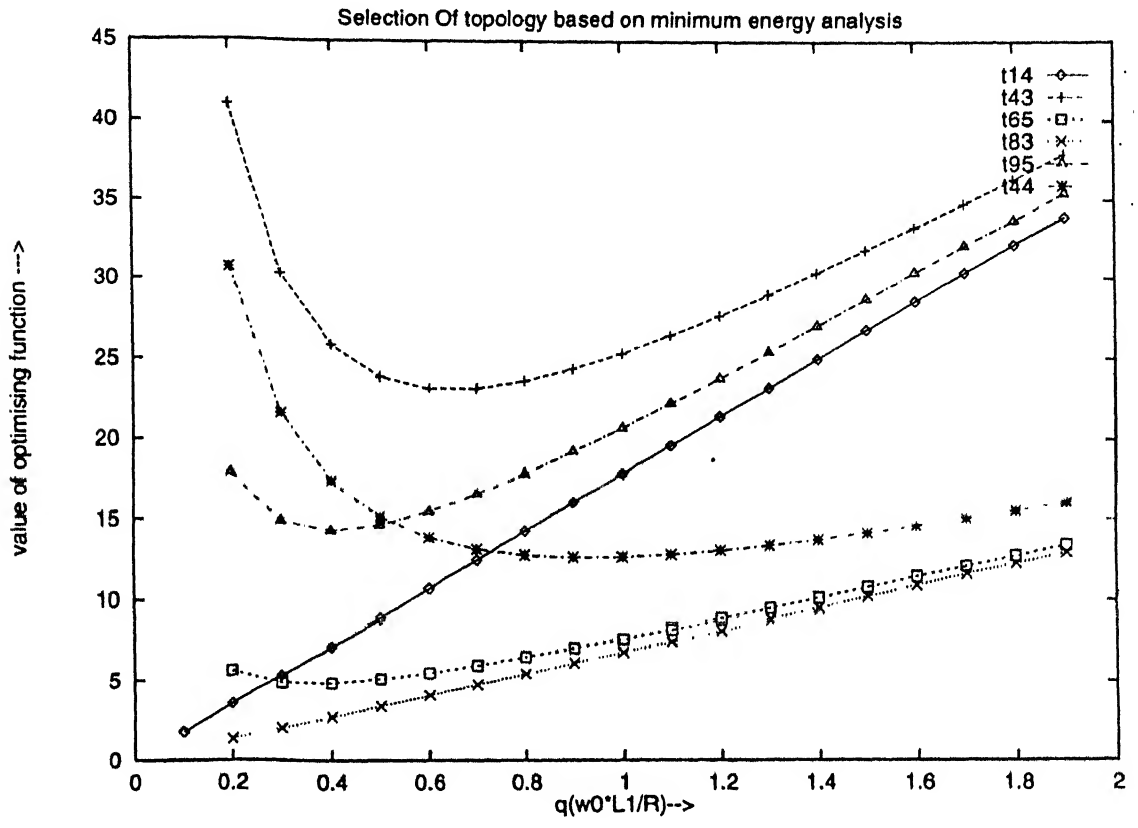

Figure 3.2: Value of Optimising function for different values of q,D=1,a = 1, b = 1.

of the S2 and hence is fit for further consideration. Whereas for the case $a = 1, b = 2$ (fig. 3.5), Topology 65[13] offers the minimum value of S2. Topology 83 which is number given in [13] which is same as the topology 8 of this work,which has been used for presentation of concepts so far. Hereafter topology 8 will be used for further description and simulation studies.

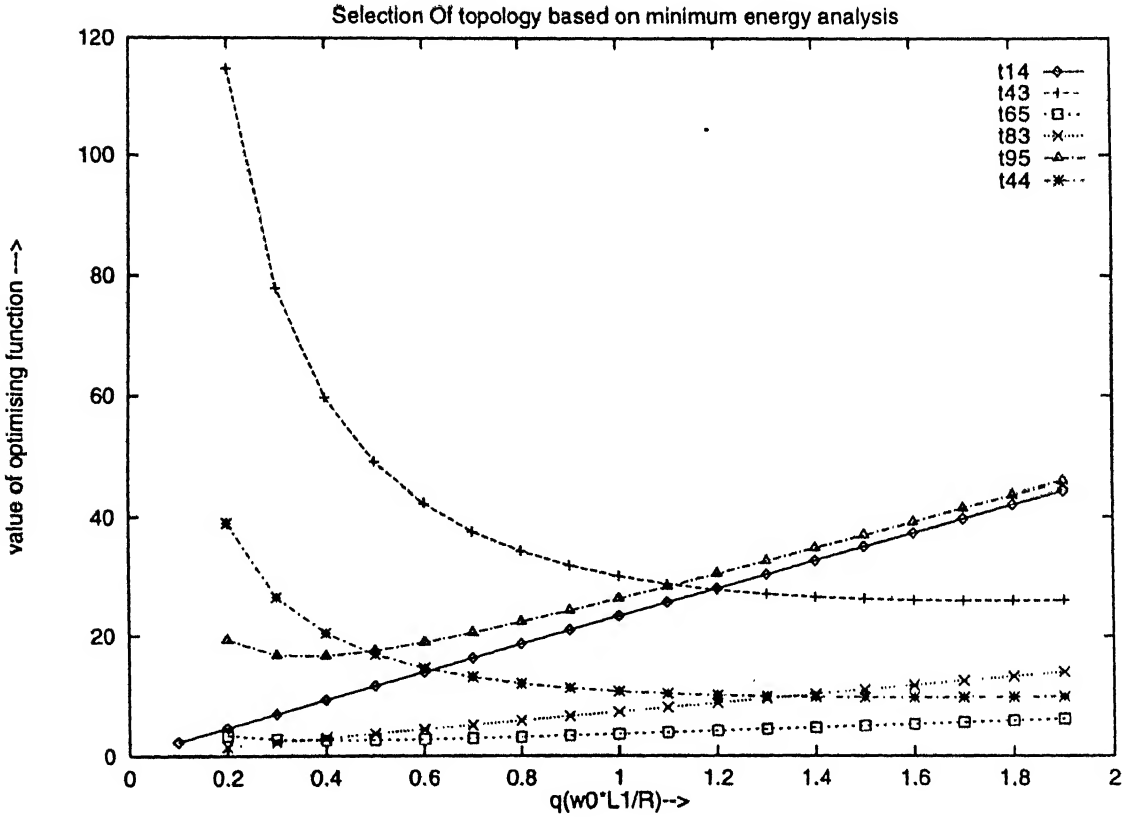

Figure 3.3: Value of Optimising function for different values of q,D=1,a = 2, b = 2.

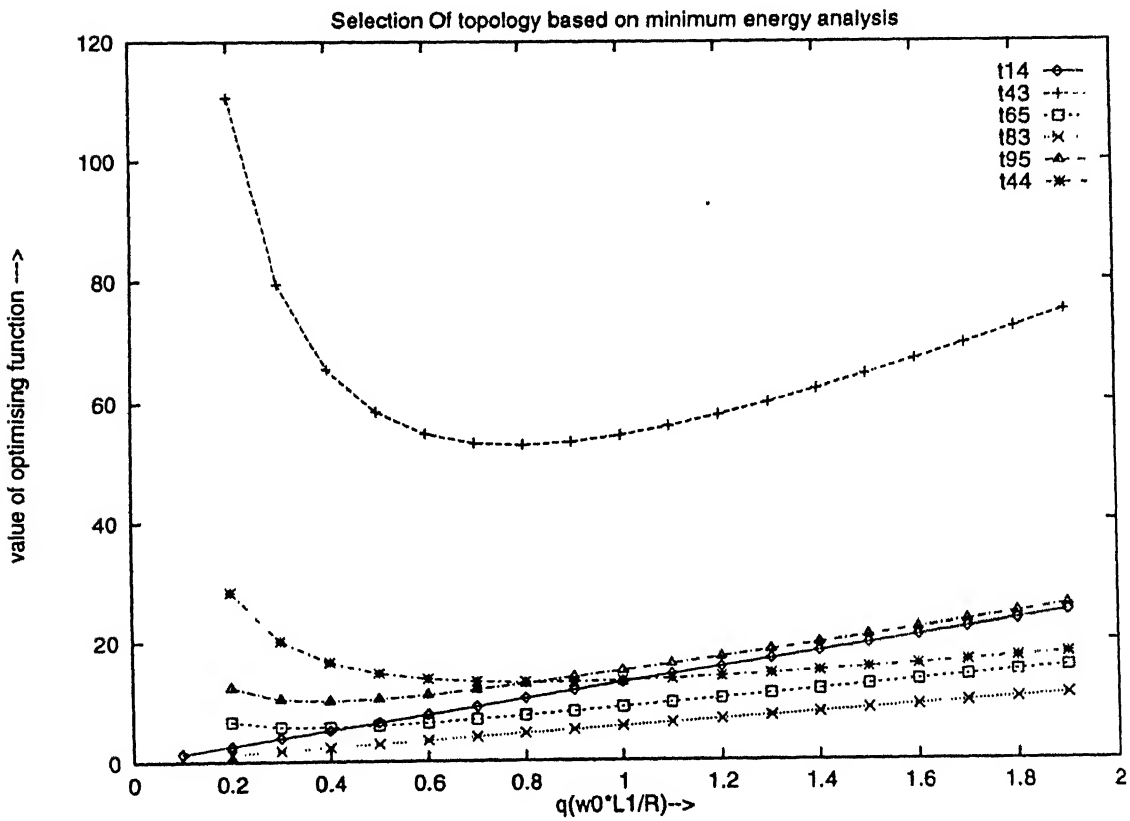

Figure 3.4: Value of Optimising function for different values of q,D=1,a = 2, b = 1.

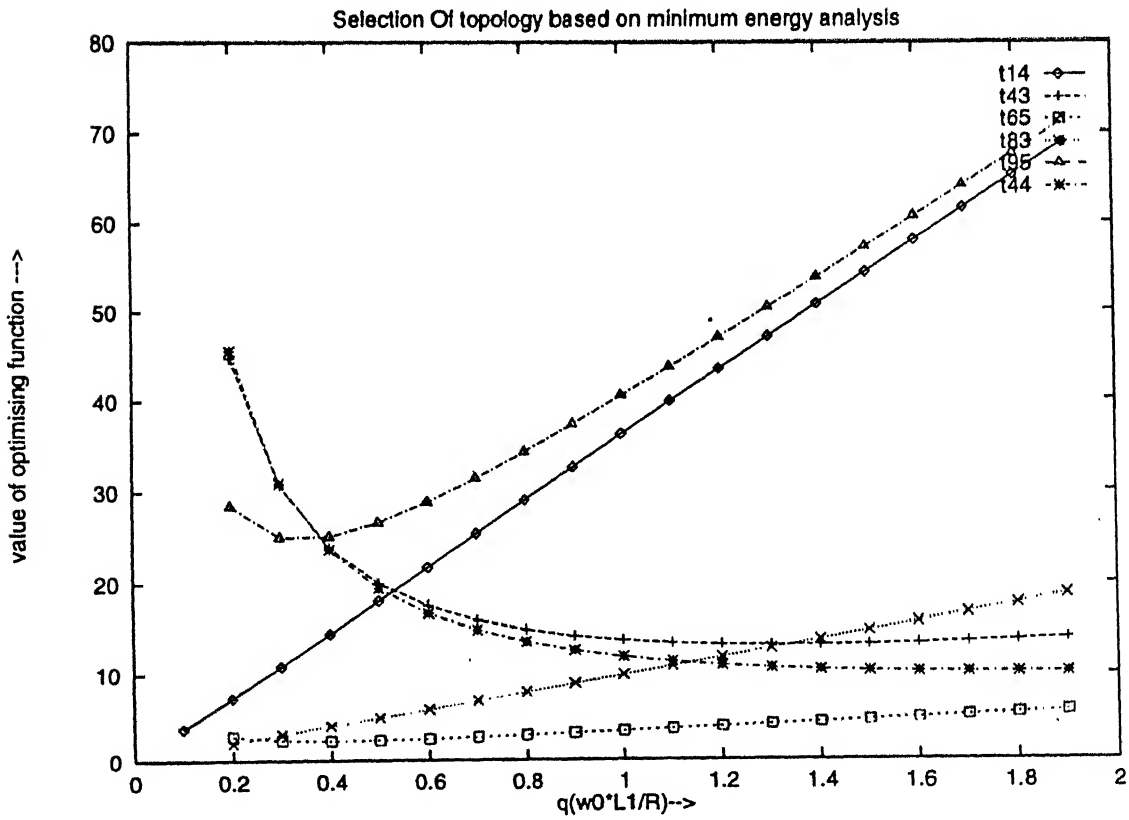

Figure 3.5: Value of Optimising function for different values of q,D=1,a = 1,b = 2.

Chapter 4

LCLC Converter

4.1 Description of Circuit Functioning

Fig 4.3 shows simplified version of full bridge LCLC converter and fig. 4.2 shows the timing trigger sequence for the IGBT's. The IGBT's are driven at slightly less than 50% of duty cycle to avoid simultaneous conduction of the devices of same leg. All the IGBT's are gated by a clock signal whose frequency determines the switching frequency ω_s of the converter . IGBTS' S_{12} and S_{22} are gated with a controllable time delay (τ) with respect to the gating of S_{11},and S_{21} respectively. The input voltage v_{AB} to the resonant converter,the current i_{L1} through the series connected elements,and the reflected load voltage and current i_{L2} are shown in Fig. 4.3.The time delay(τ) is the interval during which the voltage v_{AB} (Fig. 4.3) is either $+V_s$ or -V_s,and v_{AB} remains zero during the remaining period. By varying this time delay (τ),the output voltage of the converter is controlled.

Typical voltage and current waveforms of the resonant tank are shown in Fig. 4.3 represent all the state variables. The input and output switching voltages are also included in fig. 4.3. The switching frequency ω_s is selected to be ω_{o2} given by eq. 3.7,for load independent operation. At $t = t_0$, the switch S_{11} is turned on and the switch S_{12} is turned off. If the current at t_0 is positive it will represent leading pf operation and if the current is negative then it will be lagging pf operation. Here lagging pf operation is assumed. Since the current i_{L1} at $t = t_0$ is negative,the diodes D_{11} and D_{12} conduct till i_{L1} becomes zero,v_{AB} is equal to $+V_s$. At $t = t_1$,the current i_{L1} becomes zero and begin to go positive , hence the switch pair $S_{11}S_{22}$ conduct upto $t = t_2$. The interval

$(t_2 - t_1)$ is called power interval during which the input source supplies tank as well as load energy. The period $(t_1 - t_0)$ is the regenerative interval, in which the tank circuit returns energy to the input supply, while supplying the load energy. At $t = t_2$,the switch S_{22} is turned off and S_{12} is turned on. The current i_{L1} freewheels through S_{11},resonant tank and D_{12}. This continues upto $t = t_3$ and the interval $(t_3 - t_2)$ is called free resonant interval. During this interval, the resonant tank supplies energy to the load and no energy is supplied to the input source. At $t = t_3$ the switch S_{11} is gated off and S_{21} is turned on. Since the half cycle stability and odd symmetry of the converter is to be maintained hence the states at $t = t_3$ are same with opposite polarity as those at $t = t_0$,in steady state. Hence the diodes D_{21} and D_{12} conduct till the current becomes zero at $t = t_4$,this interval is again regenerative period similar to the interval $(t_1 - t_0)$ in the begining. From $t = t_4$ to $t = t_5$, the switch $S_{12}S_{21}$ conduct constituting the second power interval in a cycle. At $t = t_6$,S_{12} is turned off and S_{22} is turned on. S_{21} and D_{22} conduct giving the free resonant interval from t_6 to t_7. The waveforms shown for one complete cycle repeat again.

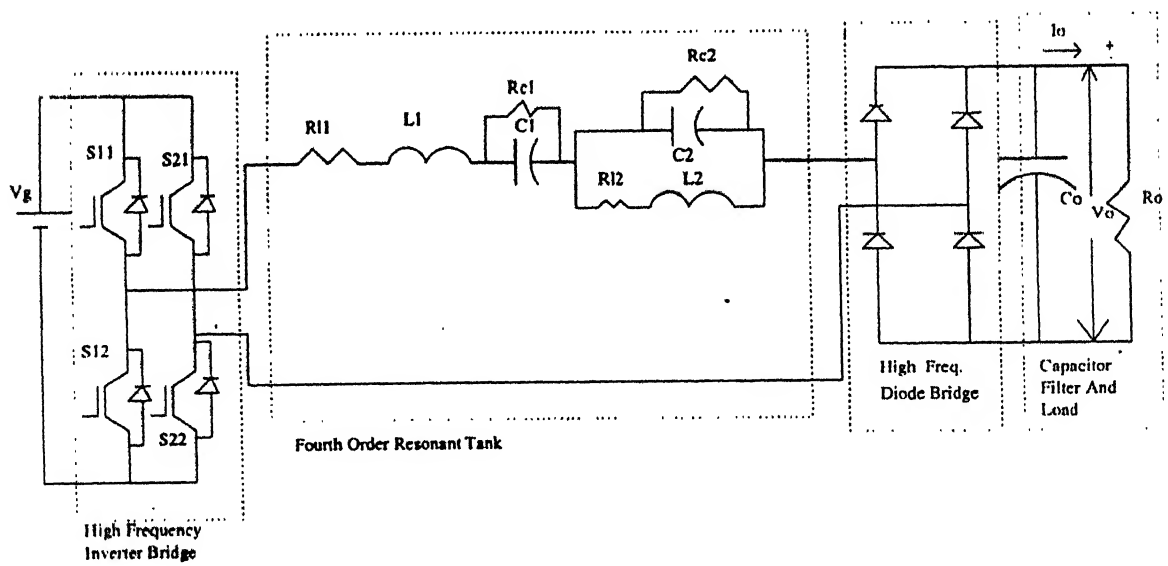

Figure 4.1: The circuit diagram of a fourth order resonant converter

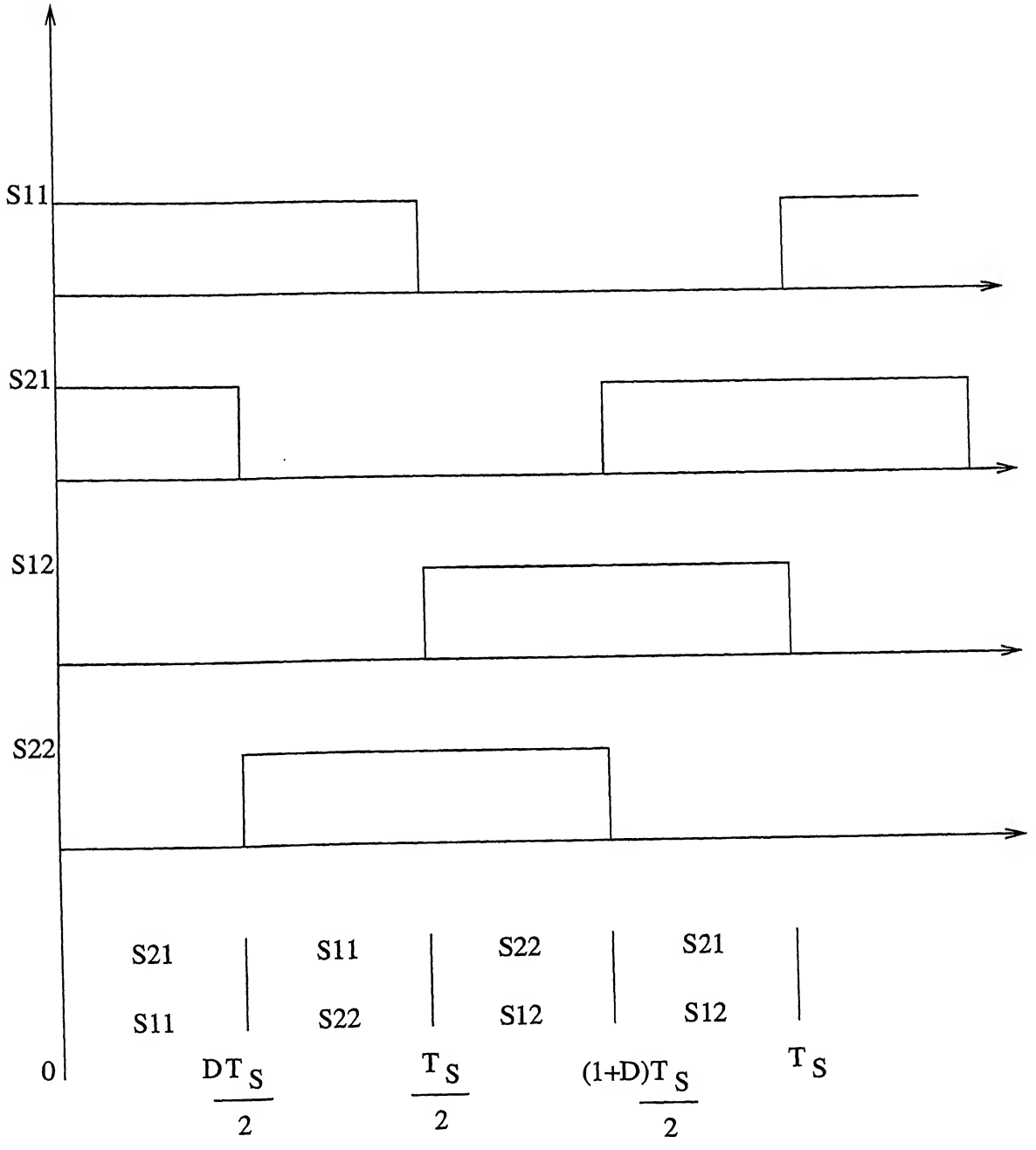

Figure 4.2: Switching (Gate) wave forms for the different switches of high frequency inverter.

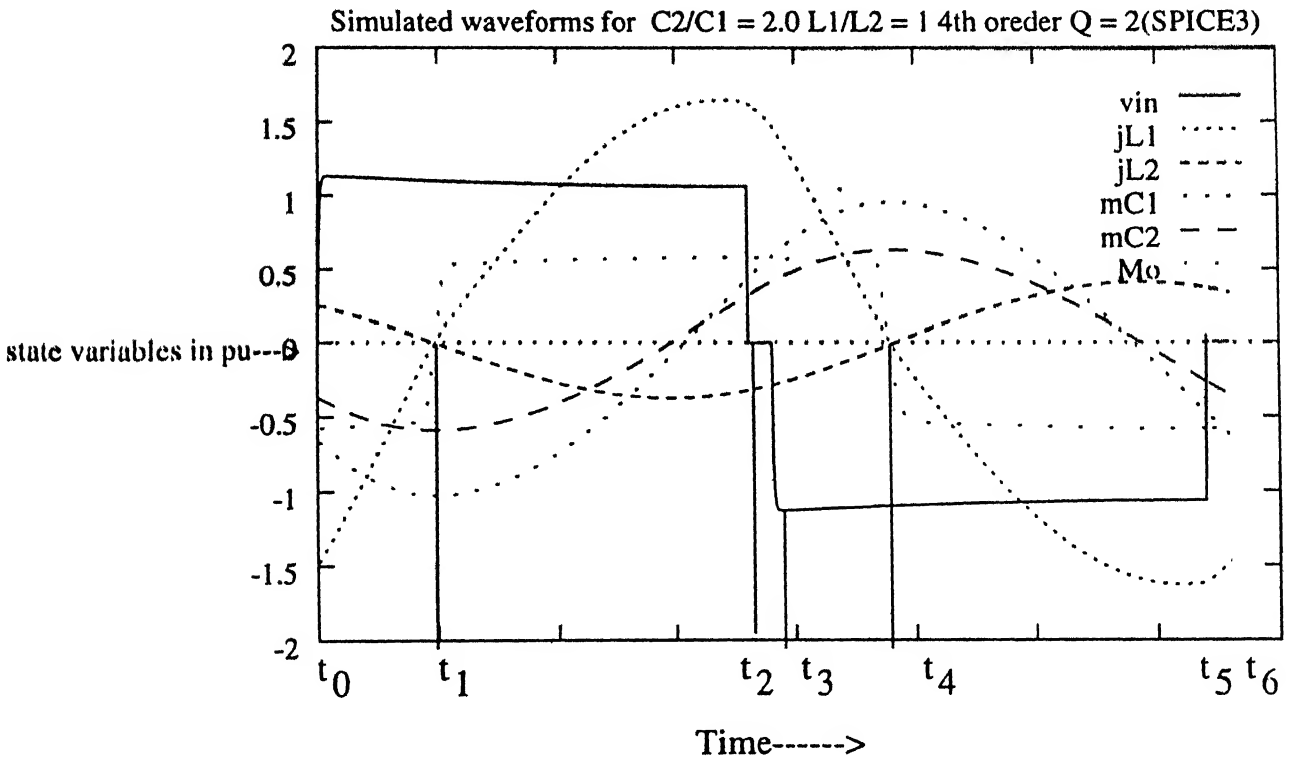

Figure 4.3: Timing Diagram of the state variables(Normalised) of the conveter(Lagging pf mode

Chapter 5

Simulation Of the Converter

5.1 Introduction

In this chapter the fourth order converter topology obtained in chapter 4 is extensively simulated and the simulated values are compared with those obtained by analysis. The simulation of the converter by SPICE3 software package is a time consuming exercise and also the results are not presented in a format which can be used for evaluating the parameters like components stresses etc. .

A C program is written to simulate the different converters by solving the differntial equations and also taking care of the parasitics of the components. The results obtained by this simulation method and those obtained by SPICE3 simulation are compared and found to be matching.

Design methodology of the converter is also suggested in this chapter.

5.2 Design of the Converter Components

The converter design is carried out around following specifications:

- Minimum input DC voltage V_s: 50 V.
- Maximum output voltage: 50 V.

- Max Output current: 2 A.
- Maximum overload current: 4 A.
- switching frequency: 100 KHz.
- Max ripple of output voltage: 2%.
- $\frac{C2}{C1} = 2, \frac{L1}{L2} = 1.$

The design process is presented as following:

1. Select the operating frequency to be ω_{o_2}.
   $\omega_{o_2} = \frac{1.31}{\sqrt{L1C1}}$ for $a = 2$ and $b = 1$.

$$\omega_{o_2} = 2\pi 100 * 10^3 \tag{5.1}$$

$$\frac{1}{L1C1} = \left(\frac{\omega_{o_2}}{1.31}\right)^2 = 2.3 * 10^{11} \tag{5.2}$$

$$L1C1 = 4.35 * 10^{-12} \tag{5.3}$$

$$Q_{1max} = \left\{\frac{\sqrt{\frac{L1}{C1}}}{\left(\frac{V_o}{I_{omax}}\right)}\right\} \tag{5.4}$$

2. Let the value of Q_1 corresponding to maximum overload be 4.0 to restrict the stresses on resonant components.
   $Q_{1max} = 4.0$ and $Q_{1min} = 0.4$. from eq. 5.4 we find

$$\sqrt{\frac{L1}{C1}} = 50 \tag{5.5}$$

3. Using eq. 5.3- 5.5 we can find the values of $L1$ and $C1$ respectively. By using the values of a and b we can find the values of $C2$ and $L2$ respectively.

   $L1 = 104\mu H \; C1 = 0.042\mu F$

4. Let us choose the value of $C1$ to be $0.04\mu F$ because $0.01\mu F$ capacitors are available easily and four such capacitors can be paralleled together.

5. Now the value of $L1$ and $L2$ is modified to be $L2 = L1 = 100\mu H$ and $C2 = 0.08\mu F$.

6. The new operating frequency is found to be

$\omega_{o2} = \frac{\frac{1.31}{\sqrt{L_1 C_1}}}{2\pi} = 104KHz.$

5.2.1 Selection of the Output Filter Capacitor C_O

The obvious effect of the large filter capacitor is the reduction of the ripple in the output DC voltage of the converter but if the filter capacitor is very large then the starting transients of the converter become more severe and the resonant component stresses may go beyond the maximum limit and this may damage the switches.

Another problem of the large filter capacitor is large settling time for the transients of the converter. Hence the transient analysis of the converter becomes necessary to determine the optimum value of the filter capacitor which gives satisfactory transient response besides meeting the output voltage ripple requirements.

In fig. 5.3 the variation of the percentage ripple vs the filter capacitor is shown. It is observed from the figure that the percentage ripple increases as we increase the ratio $\frac{C_1}{C_o}$(or decrese of the filter capacitance value). If the ratio $\frac{C_1}{C_o}$ is less than or equal to 0.035 then the percentage ripple remains within the desired limit($\leq$2%).

The transient analysis of the converter is carried out on cycle basis and the peak component stresses in each cycle are treated as state variables in each cycle.

The variation of peak component stresses in response to a step change in load resistance(or Q_1) is shown in fig. 5.1 and it is observed that if $\frac{C_1}{C_o}$ is smaller(0.0035) the transient behaviour of the converter is more severe than that when $\frac{C_1}{C_o}$ is larger(0.035).

Similarily the transient behaviour in response to a step change in duty ratio(D) from D_{min}(0.4) to D_{max}(1.0) is shown in fig. 5.2 and is observed that the peak stresses and settling time are minimal in the case of larger ratio $\frac{C_1}{C_o}$(or smaller filter capacitance C_o).

Hence in the light of the above discussion the filter capacitor is selected to be such that it is smallest of those which satisfy the output ripple requirement($\leq$ 2%).

Hence $\frac{C_1}{C_o} = 0.035$ is selected and the value of filter capacitor is chosen to be $1.15\mu F$.

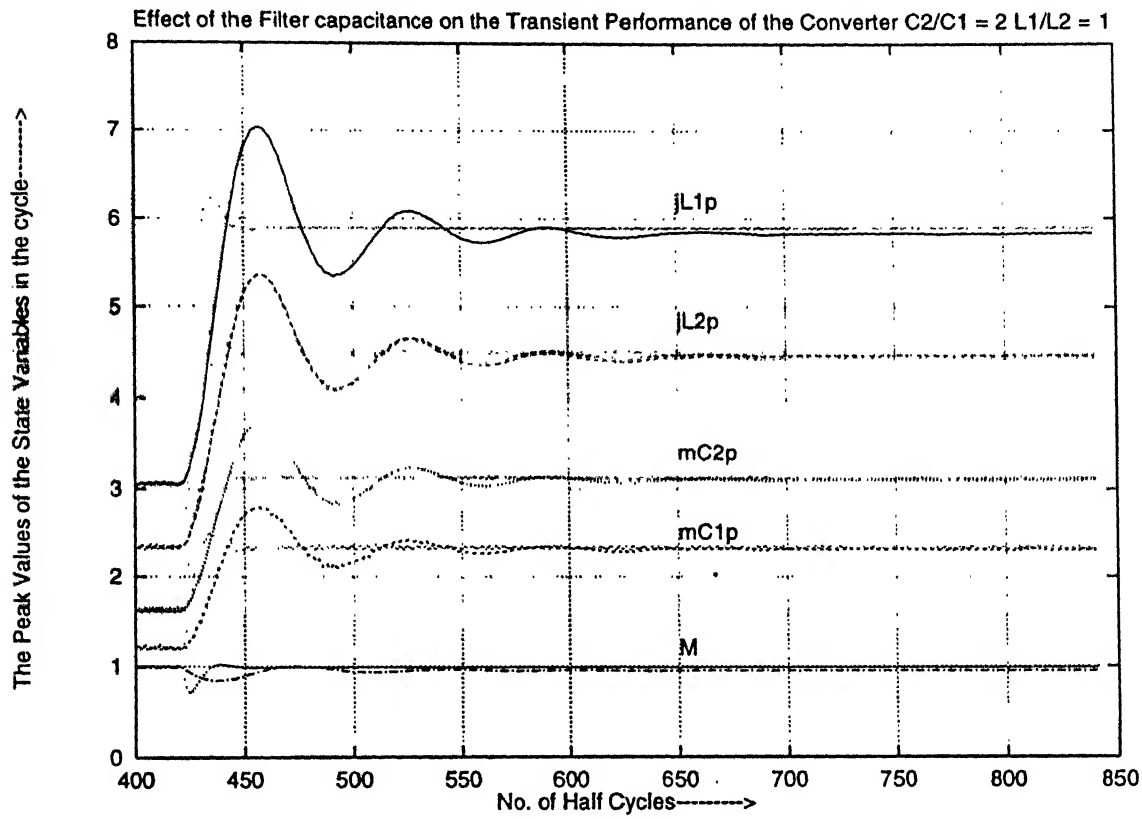

Figure 5.1: Transient response for the step change in the load resistance(from Q1=2.0 to Q1 = 4.0) with two different filter capacitors (dots for $\frac{C1}{C_o} = 0.035$ and lines for $\frac{C1}{C_o} = 0.0035$.

5.3 Start-Up of the Converter

The converter can be started with or without any charge at filter capacitor. If converter is started with zero charge on filter capacitor then the start-up transients are more severe than when it is started with some charge as observed from fig. 5.4.

5.4 SPICE3 Simulation Methodology

The SPICE3(Simulation Program with Integreted Circuit Emphasis) is used extensively for the simulation of electronic circuits. The circuit description is presented as an input file to SPICE3 and the analysis commands are also part of the input file. Fig. 5.5 gives the circuit diagram used for simulation. Current monitoring is done by inserting zero-

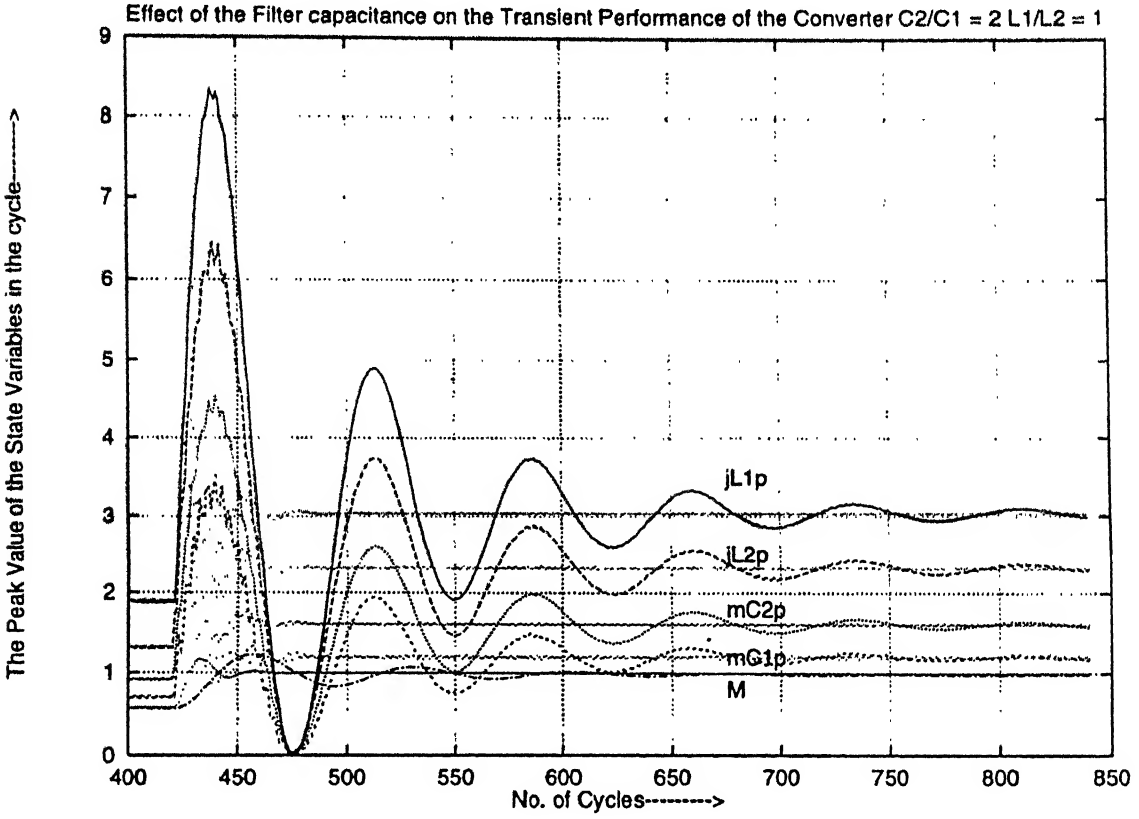

Figure 5.2: Transient response for the step change in duty ratio(from D=0.4 to D = 1.0) with two different filter capacitors (dots for $\frac{C1}{C_o} = 0.035$ and lines for $\frac{C1}{C_o} = 0.0035$

voltage sources in series with the branch. The symbol in the figure indicates the current monitoring paths. Resistances of low values are included in series with all inductors and resistaces of high values are connected in parallel with capacitances to make the simulation network more realistic and also to avoid possible reactance loops. If there is only reactance loop,then the spice3 simulation is aborted due to non-convergence. Fast recovery diodes are simulated by changing the transit time(TT) parameter of standard diode model of spice3. MOSFET mode 1 is used for simulating the active switch . The transconductance (K_p) and mobility (V_o) of the standard model is changed to get the desired characterstics of switch [25].

The analysis is carried out over a long period of time (say 20 cycles of the inverter voltage) and data is taken during the last cycle. Thus,stable steady state is established before taking the data.

The transient analysis is carried out for different duty ratios and externe load con-

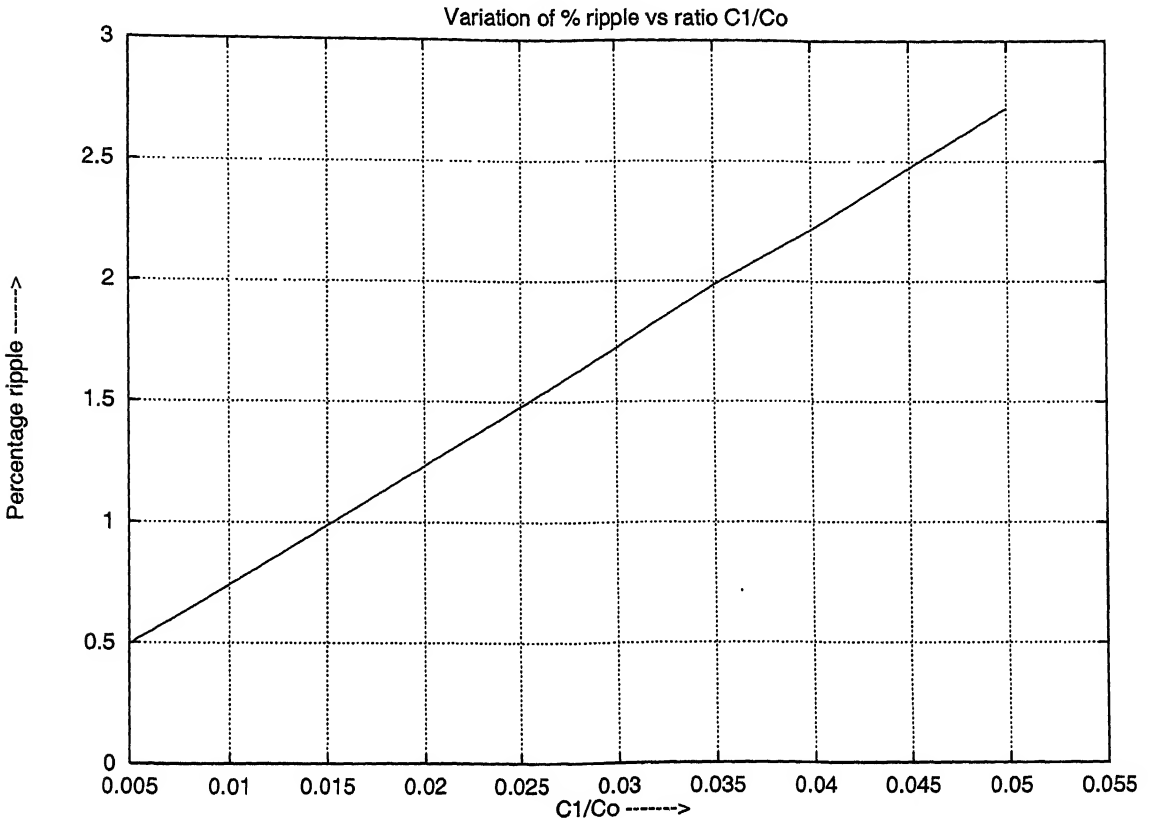

Figure 5.3: Variation of percentage ripple in output voltage vs ratio $\frac{C1}{C_o}$ (Q1 = 2.0)

itions ($Q_1 = 0.4(R_L = 125ohm)$ to $Q_1 = 2.0(R_L = 25ohm)$. Fig. 5.6- 5.11 give the mulation waveforms of all state variables,input switching waveforms,output switching waveforms . There are two sets of waveforms for each duty cycle, representing the xterme load conditions. All the variable obtained by simulation are normalised with ase values as defined in Appendix-A, for comparision purposes.

From these waveforms it is observed that the output voltage of the converter remains nstant from minimum load to maximum load(load independent operation) as it was und from the analysis. From the simulation waveforms it is observed that the converter enters into discontinuous mode for low load and low duty cycle($Q_1 = 0.4, D = 0.4$ g. 5.7).

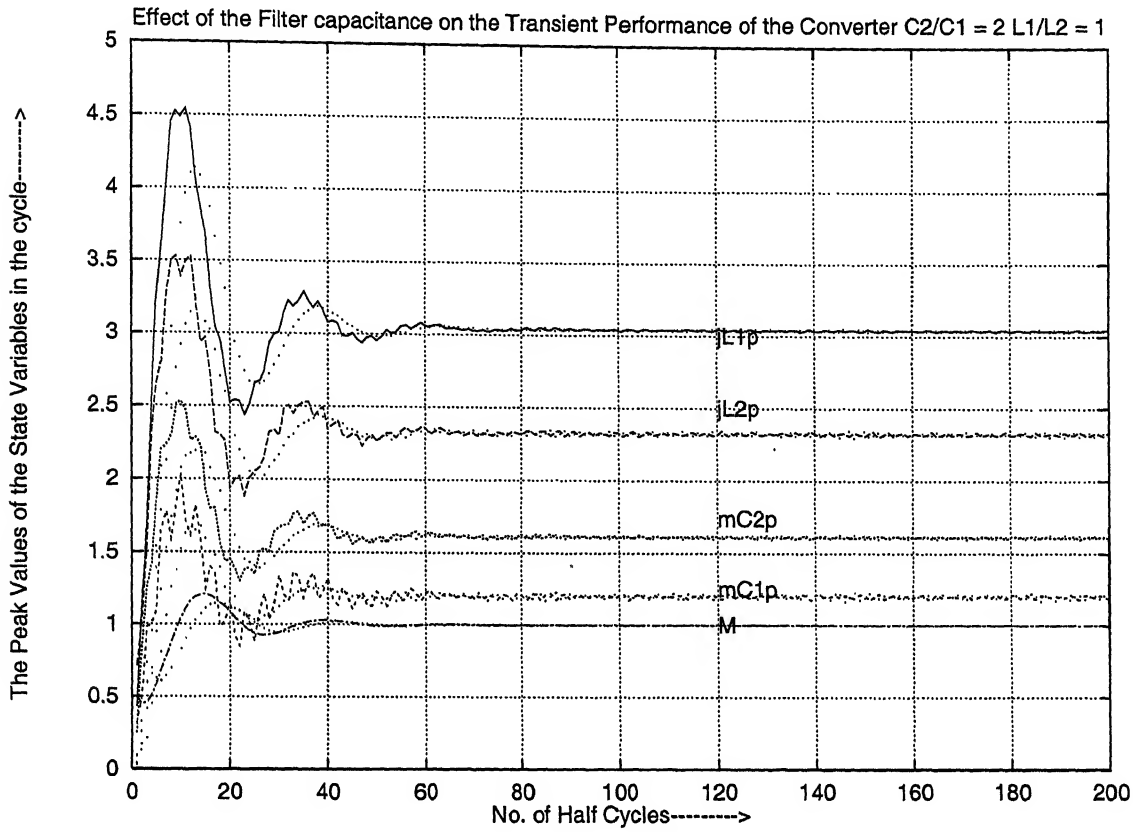

Figure 5.4: Start-up Transient response with two different filter capacitor initial voltages $\frac{C1}{C_o} = 0.035$ (dots for Mo = 1.0 and lines for Mo = 0.5)

5.5 Simulation by Transient Numerical Solution of Differential Equations

The SPICE3 does not support programming and the variables are not accessible for on-line processing. Hence for having more insight of the circuit operation and enhancing the speed of the simulation, a general C program was written which solves the converter dynamical equations using Runge-Kutta method and applying proper switching condition, for simulating the converter.

The results obtained by this program and those obtained by the SPICE3 are shown in fig. 5.12- 5.13 and it is observed that these two plots are almost matching and the rasults of the simulation by C program are validated. The same C program is used for transient analysis of the converter as discussed in section 5.2.1.

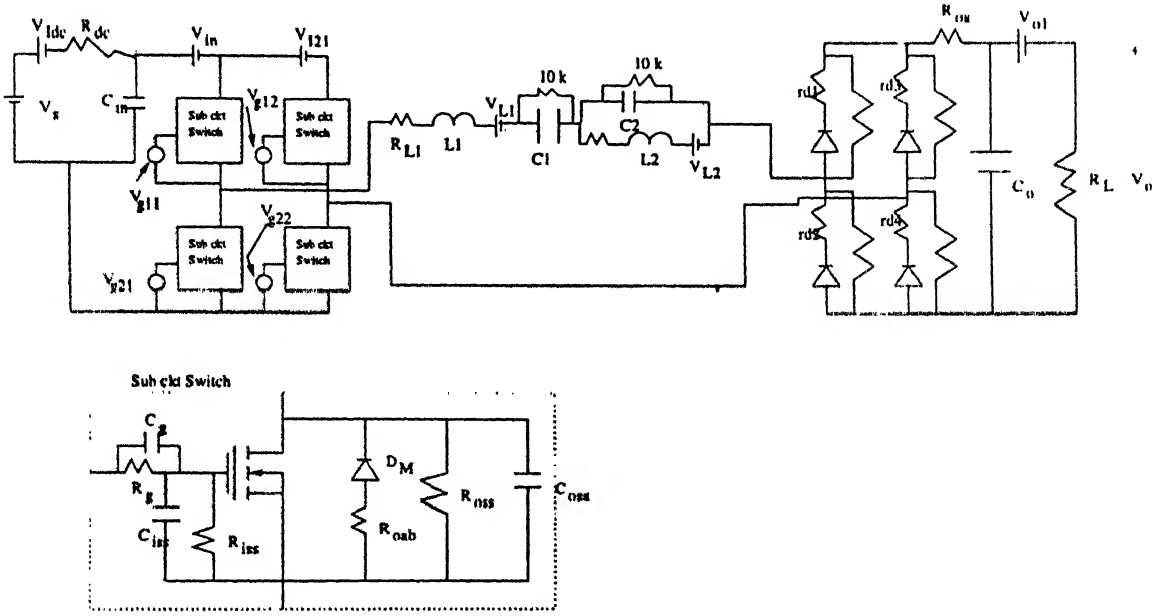

Figure 5.5: Detailed Circuit Diagram of the Converter Used for SPICE3 Simulation(Topology 8)

5.5.1 Operation of the Converter with Pulsed Load

The converter performance with pulsed load is important to study the dynamics of the converter. With pulsed loads the converter can take large instantaneous stresses without being overloaded. The converter's performance with pulsed load is tested using C program and changing the load resistance at the end of every half cycle. The converter wave forms with pulsed load are shown in fig. 5.14.

From the fig. 5.14 it is observed that for pulsed load the ripple in the output voltage is increased to a large extent depending on the differece between minimum and maximum loads.

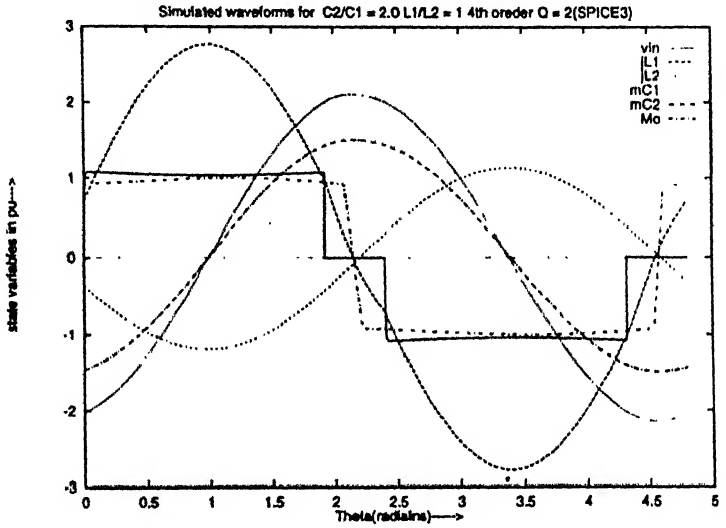

Figure 5.8: Simulated wave forms for $Q_1 = 2(R_L = 25ohm)$ D = 0.8.

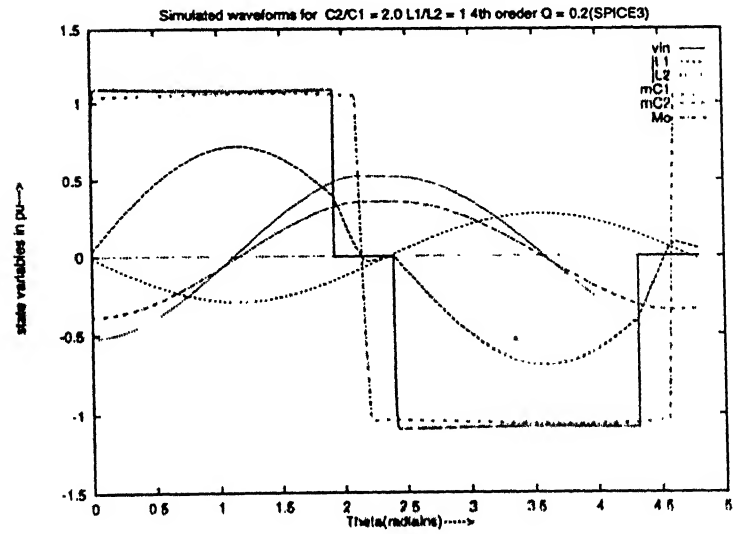

Figure 5.9: Simulated wave forms for $Q_1 = 0.4(R_L = 125ohm)$ D = 0.8.

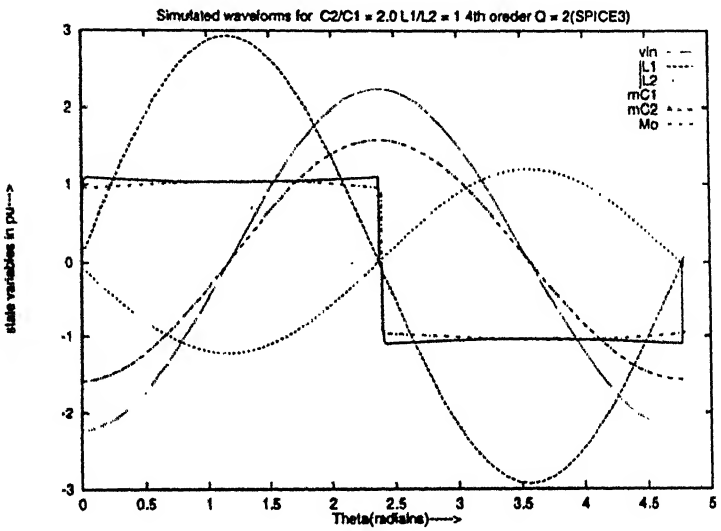

Figure 5.10: Simulated wave forms for $Q_1 = 2(R_L = 25ohm)$ D = 1.0.

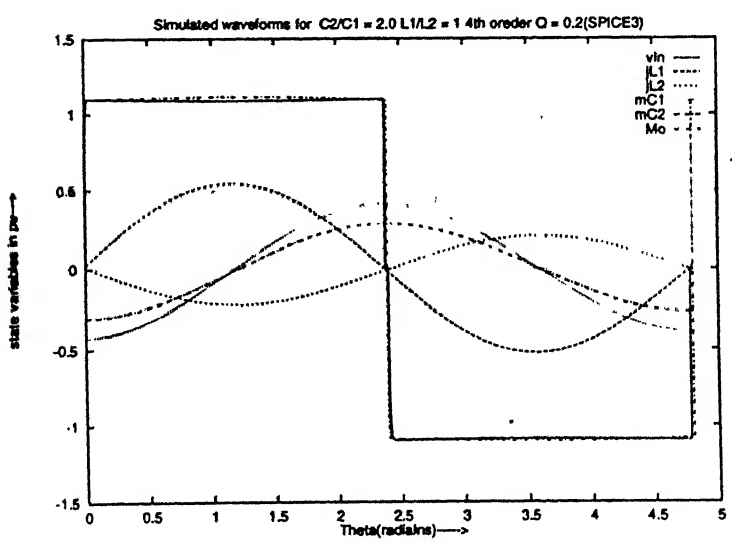

Figure 5.11: Simulated wave forms for $Q_1 = 0.4(R_L = 125ohm)$ D = 1.0.

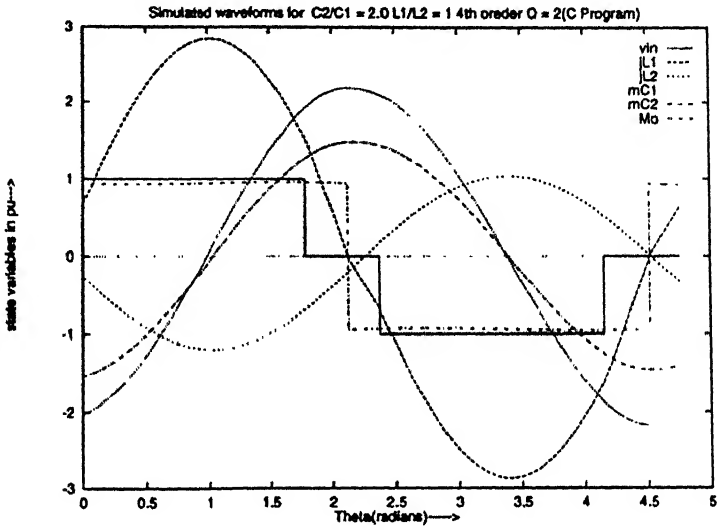

Figure 5.12: Simulation Waveforms of the Converter for $Q_1 = 2.0$,D $= 0.75$(Using C program).

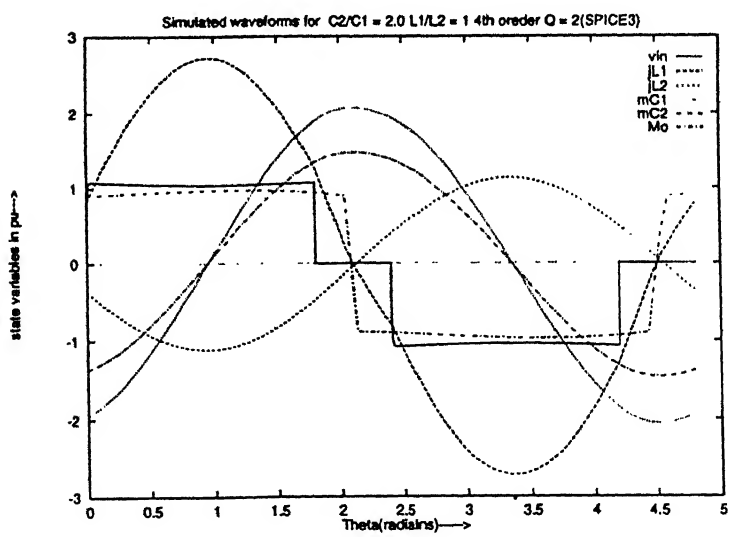

Figure 5.13: Simulation Waveforms of the Converter for $Q_1 = 2.0$,D $= 0.75$(Using SPICE).

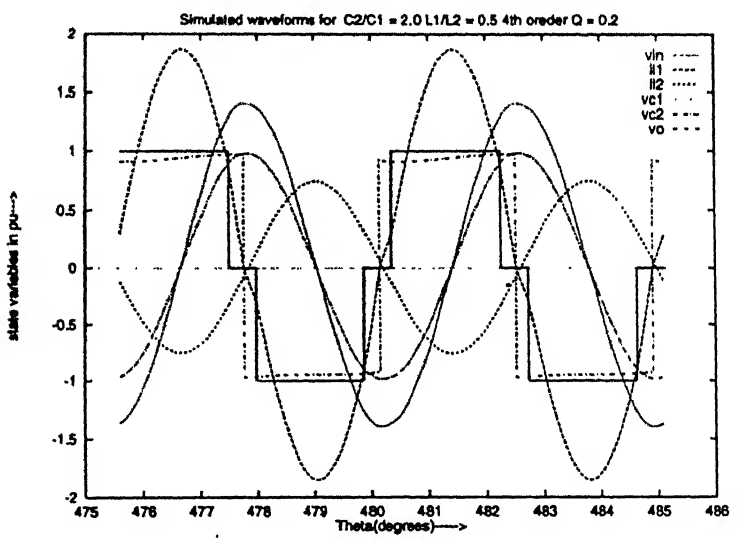

Figure 5.14: Simulated Waveforms of the State variables for Pulsed Load($Q_{1min} = 0.5, Q_{1max} = 2.0, D = 0.8$).

Chapter 6

Conclusion

6.1 Conclusion

The analysis and simulation of fourth order resonant DC-DC convreters with capacitive filter at output has been proposed and studied. The analysis of the fourth order converters has been carried out with a new method known as state transformation method. From the analysis it was observed that all selected fourth order converters have two frequencies at which load independent operation takes place.

The selection of the topology has been based on the minimum component stress method and was applied on all the converter topologies and one offering the minimum stresses was selected for further study.

Design procedure and equations have been obtained based on the analysis and the have been used to illustrate a design example.

The exhaustive simulation of the selected topology was carried out for different operating conditions using SPICE3 software package. The simulation results are in agreement with the analytical results.

The transient behaviour of the converter are also studied by simulation, by a C program. The effect of the output filter capacitance on the transient behaviour of the converter,was also studied and optimum value of the filter capacitance is selected. The effect of the initial charge of the filter capacitor,on the starting transient behaviour of the converter is also studied and it is found that converter should be started with filter

capacitor charged to some finite voltage.

6.2 Suggestions for Future Work

In the selection of topology it was found that for some ratios(say a = 1,b = 2), topology 5 (65 of [13]) gives the minimum value for optimising function. Hence the characterstics of this topology can also be investigated in detail.

The method of state space decoupling has proved to be efficient when compared with the real time simulations run to obtain the steady state solutions,hence this method can be extended to the analysis of other converters and also for different control methods of the same converter.

Possibility of closed loop robust controllers to make the dynamic performance superior can also be explored.

Bibliography

[1] A.F.Witulski,R.W.Erickson,"Design of the Series Resonant Converter for Minimum Component Stress",*IEEE Trans. on Aerospace and Electronic Syst.*,Vol. 22,No. 4,July 1986,pp. 356-363.

[2] Thomas H.Sloane,"Design of High-Efficiency Series-Resonant Converters Above Resonance",*IEEE Trans. on Aerospace and Electronic Syst.*,Vol. 26,No. 2,March 1990,pp. 393-402.

[3] I.Batarseh,"State-plane Approach for the Analysis of Half-bridge Parallel Resonant Converters",*IEE Proc.-Circuits Devices Syst.*,Vol. 142,No. 3,June 1995,pp. 200-204.

[4] I.Batarseh,C.Q.Lee,"Steady-State Analysys of the Parallel Resonant Converter with LLCC-Type Commutation Network", *IEEE Trans. on Power Electron.*,vol.6,No.3 ,July 1991,pp. 525-538.

[5] Ashoka K.S.Bhat,"Analysis and Design of a Series-Parallel Resonant Converter" ,*IEEE Trans. on Power Electron.*,vol.8,No.1,Jan 1993,pp. 1-11.

[6] K.Natarajan,S.Sivakumar,"Optimal Trajectory Control Of Constant Frequency Series Resonant Converter",*Proc. of PESC'93*,pp. 215-221.

[7] Z.Q.Wang,I.Batarseh,J.Bu,"Robust Controller Design for a Series Resonant Converter" ,*IEEE Trans. on Aerospace and Electronic Systems*,vol.32,No. 1,Jan1996,pp.221-232.

[8] R.Oruganti,T.C.How,"Resonant-Tank Control of Parallel Resonant Converter", *IEEE Trans. on Power Electron.*,Vol.8,No.2,Apr.1993,pp127-134.

[9] Gorge C. Verghese,Malik E. Elbuluk,and John G. Kassakian,"A General Approach to Sampled-Data Modeling fo Power Electronic Circuits",*IEEE Trans. on Power Electron.*,Vol. 1,No. 2,Apr. 1986,pp. 76-89.

[10] A.J.Forsyth,Y.K.E.Ho,"Dynamic characterstics and closed-loop performance of the series-parallel resonant converter",*IEE Proc.-Electr. Power Appl.*,Vol.143,No.5 ,Sept199 6,pp. 345-353.

[11] R.Liu,C.Q.Lee,"Series Resonant Converter with Third-Order Commutation Network", *IEEE Trans. on Power Electron.*,Vol.7,No.3,Jul1992,pp. 462-468.

[12] Marian K. Kazimierczuk,"Phase Control of Series Resonant Converter",*Proc. of PESC'93*,pp. 1002-1008.

[13] I.Batarseh,"Resonant Converter Topologies with Three and Four Energy Storage Elements" ,*IEEE Trans. on Power Electron.*,Vol.9,No.1,Jan. 1994,pp. 64-73.

[14] Woo H. Kwon and Gyu H. Cho,"Optimum Quantum Sequence Control of Quantum Series Resonant Converter for Minimum Output Voltage Ripple" ,*IEEE Trans. on Power Electron.*,Vol.9,No.1,Jan. 1994,pp. 74-83.

[15] Byeong-Rim Jo,Hee-Wook Ahn,Gun-Woo Moon,Hyun-Chil Choi,and Myung-Joong Youn,"Decoupled Output Voltage Control of Quantum Series Resonant Converter for Improved Buck-Boost Operation" ,*IEEE Trans. on Power Electron.*,Vol.11,No.1,Jan. 1996,pp. 147-161.

[16] Junanyu Bu,M.Sznaier,Z.Q.Wang,and I.Batarseh,"Robust Controller Design for a Parallel Resonant Converter Using μ -Synthesis" ,*IEEE Trans. on Power Electron.*,Vol.12,No.5,Sep. 1997,pp. 837-853.

[17] S.C.Wong,and A.D.Brown,"Parallel resonant converter as a circuit simulation primitive" ,*IEE Proc.-Circuits Devices Syst.*,Vol. 142,No. 6,Dec. 1995,pp. 379-386.

[18] C.Q.Lee,and K.Siri,"Analysis and Design of Series Resonant Converter by State-Plane Diagram",*IEEE Trans. on Aerospace and Electronic Sys.*,Vol. 22,No. 6,Nov. 1986, pp. 757-763.

[19] H.M.Suryawanshi,and S.G.Tarnekar,"Modified LCLC-type series resonant converter with improved performance",*IEE Proc.-Electr. Power Appl.*,Vol. 143,No. 5,Sep. 1996, pp. 354-360.

[20] V.Vorperian,and Slobodan Cuk,"A Complete DC Analysis of The Series Resonant Converter" ,*IEEE-PESC'82*,Jun. 1982,pp. 85-100.

[21] Francisc C.Schwarz,"An Improved Method of Resonant Current Pulse Modulation for Power Converters",*IEEE Trans. on Ind. Electron. and Control Instrumentation*,Vol. 23,No. 2,May 1976,pp. 133-141.

[22] Khai D.T. Ngo,"Analysis of a Series Resonant Converter Pulsewidth Modulation or Current Controlled for Low Switching Loss",*IEEE Trans. on Power Electron.*, Vol. 3,No. 1,Jan. 1988,pp.

[23] Hyun C. Choi,and M.J. Youn,"A Soft-Switched,High-Frequency Resonant Rectifier and Characterstics of the Controlled System",*IEEE Trans. on Power Electronics*,Vol. 12,No. 1,Jan. 1997,pp. 161-172.

[24] H.Pollock,and John O. Flower,"New Method of Power Control for Series-Parallel Load-Resonant Converters Maintaining Zero-Current Switching and Unity Power Factor Operation.",*IEEE Trans. on Power Electronics*,Vol. 12, No. 1,Jan. 1997,pp. 103-115.

[25] G.S.N.Raju,"A New LCL Resonant Converter with PWM Control",*M.Tech. Thesis submitted to Deptt. of EE,IIT Kanpur*,Feb. 1993.

[26] M.Ramachandra Rao,"Analysis,Simulation,Design and Implementation of LCC Resonant DC to DC Converter",*M.Tech. Thesis submitted to Deptt. of EE,IIT Kanpur*,May 1994.

[27] Jung-Chien Li and Yan-Pei Wu,"Closed-Form Expressions for the Frequency-Domain Model of the Series Resonant Converter",*IEEE Trans. on Power Electron.*,Vol. 5,No. 3,July 1990,pp. 337-345.

[28] Steven D. Johnson and Robert W. Erickson,"Steady-state Analysis and Design of the Parallel Resonant Converter",*IEEE Power Electronics Specialists Conf. 1986*,pp. 1-12.

[29] S.D.Johnson,A.F.Witluski,and R.W.Erickson,"A Comparision of Resonant Topologies in High Voltage DC Applications",*IEEE Applied Power Electronics Conference Record 1987*,pp. 1-12.

Appendix A

State space equations for different topologies

The state space description of all the selected topologies are given in circuit parameter form and also in the normalised form as following.

The normalisation of the variables is carried out using the following base quantities.
$V_B = V_s$

$Z_B = \sqrt{\frac{L1}{C1}}$

$I_B = \frac{V_B}{I_B}$

$\omega_B = \frac{1}{\sqrt{L1C1}}$

$\theta = \omega_B t$

$j_{L1} = \frac{i_{L1}}{I_B}$

$j_{L2} = \frac{i_{L2}}{I_B}$

$m_{C1} = \frac{v_{C1}}{V_B}$

$m_{C2} = \frac{v_{C2}}{V_B}$

$M_o = \frac{V_o}{V_B}$

Topology 2:

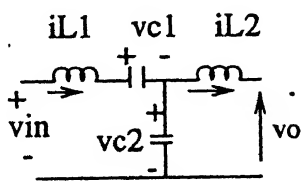

Equations in General form

$\frac{di_{L1}}{dt} = -\frac{1}{L1}(v_{C1} + v_{C2} - v_s)$
$\frac{dv_{C1}}{dt} = \frac{1}{C1} i_{L1}$
$\frac{di_{L2}}{dt} = \frac{1}{L2}(v_{C2} - v_{o1})$
$\frac{dv_{C2}}{dt} = \frac{1}{C2}(i_{L1} - i_{L2})$
$i_d = i_{L2}$

Equations in normalised form

$\frac{dj_{L1}}{d\theta} = -(m_{C1} + m_{C2} - v_{s_n})$
$\frac{dm_{C1}}{d\theta} = j_{L1}$

$$\frac{dj_{L2}}{d\theta} = b(m_{C2} - m_{o1})$$
$$\frac{dm_{C2}}{d\theta} = \frac{(j_{L1} - j_{L2})}{a}$$
$$j_d = j_{L2}$$

Topology 3:

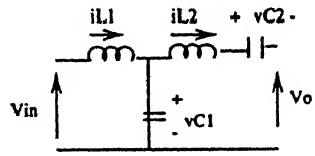

Equations in General form

$$\frac{di_{L1}}{dt} = -\frac{1}{L1}(v_{C1} - v_s)$$
$$\frac{dv_{C1}}{dt} = \frac{1}{C1}(i_{L1} - i_{L2})$$
$$\frac{di_{L2}}{dt} = \frac{1}{L2}(v_{C1} - v_{C2} - v_o)$$
$$\frac{dv_{C2}}{dt} = \frac{1}{C2}i_{L2}$$
$$i_d = i_{L2}$$

Equations in normalised form

$$\frac{dj_{L1}}{d\theta} = -(m_{C1} - v_{s_n})$$
$$\frac{dm_{C1}}{d\theta} = (j_{L1} - j_{L2})$$
$$\frac{dj_{L2}}{d\theta} = a(m_{C1} - m_{C2} - m_{o1})$$
$$\frac{dm_{C2}}{d\theta} = \frac{j_{L2}}{a}$$
$$j_d = j_{L2}$$

Topology 5:

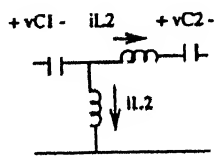

Equations in General form

$$\frac{di_{L1}}{dt} = -\frac{1}{L1}(v_{C1} - v_s)$$
$$\frac{dv_{C1}}{dt} = \frac{1}{C1}(i_{L1} + i_{L2})$$
$$\frac{di_{L2}}{dt} = -\frac{1}{L2}(v_{C1} + v_{C2} + v_{o1} - v_s)$$
$$\frac{dv_{C2}}{dt} = \frac{1}{C2}i_{L2}$$

$i_d = i_{L2}$

Equations in normalised form

$\frac{dj_{L1}}{d\theta} = -(m_{C1} - v_{s_n})$
$\frac{dm_{C1}}{d\theta} = (j_{L1} + j_{L2})$
$\frac{dj_{L2}}{d\theta} = -b(m_{C1} + m_{C2} - v_{s_n} + m_{o1})$
$\frac{dm_{C2}}{d\theta} = \frac{j_{L2}}{a}$
$j_d = j_{L2}$

Topology 7:

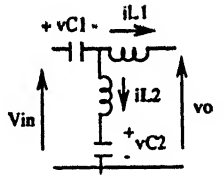

Equations in General form

$\frac{di_{L1}}{dt} = -\frac{1}{L1}(v_{C1} + v_{o1} - v_s)$
$\frac{dv_{C1}}{dt} = \frac{1}{C1}(i_{L1} + i_{L2})$
$\frac{di_{L2}}{dt} = -\frac{1}{L2}(v_{C1} + v_{C2} - v_s)$
$\frac{dv_{C2}}{dt} = \frac{1}{C2} i_{L2}$
$i_d = i_{L1}$

Equations in normalised form

$\frac{dj_{L1}}{d\theta} = -(m_{C1} + m_{o1} - v_{s_n})$
$\frac{dm_{C1}}{d\theta} = (j_{L1} + j_{L2})$
$\frac{dj_{L2}}{d\theta} = -b(m_{C1} + m_{C2} - v_{s_n})$
$\frac{dm_{C2}}{d\theta} = \frac{j_{L2}}{a}$
$j_d = j_{L1}$

Topology 8:

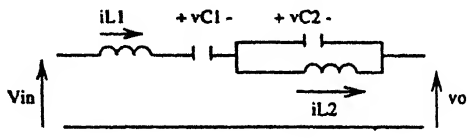

Equations in General form

$$\frac{di_{L1}}{dt} = -\frac{1}{L1}(v_{C1} + v_{C2} + v_{o1} - v_{in})$$
$$\frac{dv_{C1}}{dt} = \frac{1}{C1} i_{L1}$$
$$\frac{di_{L2}}{dt} = \frac{1}{L2} v_{C2}$$
$$\frac{dv_{C2}}{dt} = \frac{1}{C2}(i_{L1} - i_{L2})$$
$$i_d = i_{L1}$$

Equations in normalised form

$$\frac{dj_{L1}}{d\theta} = -(m_{C1} + m_{C2} + m_{o1} - v_{s_n})$$
$$\frac{dm_{C1}}{d\theta} = j_{L1}$$
$$\frac{dj_{L2}}{d\theta} = b m_{C2}$$
$$\frac{dm_{C2}}{d\theta} = \frac{(j_{L1} - j_{L2})}{a}$$
$$j_d = j_{L1}$$

Topology 13:

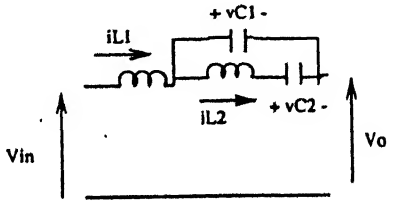

Equations in General form

$$\frac{di_{L1}}{dt} = -\frac{1}{L1}(v_{C1} + v_{o1} - v_s)$$
$$\frac{dv_{C1}}{dt} = \frac{1}{C1}(i_{L1} - i_{L2})$$
$$\frac{di_{L2}}{dt} = \frac{1}{L2}(v_{C1} - v_{C2})$$
$$\frac{dv_{C2}}{dt} = \frac{1}{C2} i_{L2}$$
$$i_d = i_{L1}$$

Equations in normalised form

$$\frac{dj_{L1}}{d\theta} = -(m_{C1} + m_{o1} - v_{s_n})$$
$$\frac{dm_{C1}}{d\theta} = (j_{L1} - j_{L2})$$
$$\frac{dj_{L2}}{d\theta} = b(m_{C1} - m_{C2})$$

$\frac{dm_{C2}}{d\theta} = \frac{j_{L2}}{a}$

$j_d = j_{L1}$

State Equation for the capacitive filter

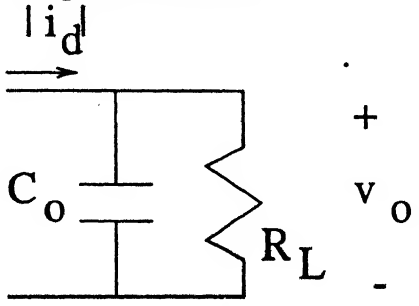

Equation in general form

$\frac{dv_o}{dt} = \frac{1}{C_o}(|i_d| - \frac{v_o}{R_L})$

Equation in normalised form

$\frac{dm_{on}}{d\theta} = c(|j_d| - Q_1 m_o)$

Appendix B

SPICE3 Program Used for Simulation of Converter(Topology 8)

```
Fourth Order LC-LC Converter
vg 2 3 dc 50v
ridc 9 4 1.0
vidc 2 9 0
vit 4 5 0
x11 5 110 1 mrf330
x12 6 120 0 mrf330
x21 1 210 3 mrf330
x22 0 220 3 mrf330
vi21 5 6 0
vg11 110 1 pulse(0 10 1n 1n 1n 4.8u 9.6u)
vg12 120 0 pulse(0 10 3.6u 1n 1n 4.8u 9.6u)
vg21 210 3 pulse(10 0 1n 1n 1n 4.8u 9.6u)
vg22 220 3 pulse(10 0 3.6u 1n 1n 4.8u 9.6u)
rl1 1 511 0.5
l1 511 512 100U
vl1 512 513 0
c1 513 514 0.04U
rc1 513 514 100k
c2 514 516 .08u
rc2 514 516 100k
rl2 514 515 0.5
l2 515 510 100u
vl2 510 516 0
rdo1 516 614 0.5
rdo2 613 616 0.5
rdo3 0 615 0.5
rdo4 613 617 0.5
rd1 516 611 .1meg
rd2 516 613 .1meg
rd3 0 611 .1meg
rd4 0 613 .1meg
ro1 611 612 0.5
co 612 613 1.15u ic = 50
vo1 612 619 0
rl 619 613 10
do1 614 611 dpa
do2 616 516 dpa
do3 615 611 dpa
do4 617 0 dpa
```

```
.model irf330 nmos ( vto = 1 kp = 2 is = 1.0e-15 )
.model dpa d (tt=50n is=1e-9)
.tran .05u 105.6u 96u uic
.end


   .subckt mrf330 31 32 33
mab 31 310 33 33 irf330
dab 315 31 dpa
rdab 33 315 0.5
cd 31 33 0.005u
rd 31 33 100k
rg 32 310 50
cg 32 310 0.1u
ciss 310 33 700p
riss 310 33 1000
.ends mrf330
```

Contributions of the Thesis

1. The study of fourth order converters in general sense. So far the study on the fourth order converter has been restricted to one topology only(LCLC parallel resonant converter with Inductor filter).

2. A new method for analytical solution of the fourth order converter is suggested.

3. Minimum component stresses method is applied for a procedural selection of the suitable topology. This method has been applied for the optimal design of Series resonant converter in ref[1].

4. The simulation of the converter was carried out by SPICE3 but SPICE3 is not fit for evaluating component stresses,effect of parameter variation at one go,Gain of the converter for different frequencies. Hence a general simulation program using the solution of differntial equation.

5. Pulsed load Analysis of the converter is presented.

6. The transient analysis of the converter is carried out which normally a scarce thing in resonant converter literature.